Anode Improvement in Rechargeable Lithium-Sulfur Batteries.

AUTHOR(S)

Tao Tao, S Lu, Ye Fan, Weiwei Lei, S Huang, Ying (Ian) Chen

PUBLICATION DATE

19-06-2017

HANDLE

10536/DRO/DU:30099154

ADVANCED MATERIALS
www.advmat.de

Anode Improvement in Rechargeable Lithium–Sulfur Batteries

Tao Tao, Shengguo Lu, Ye Fan, Weiwei Lei, Shaoming Huang, and Ying Chen**

Owing to their theoretical energy density of 2600 Wh kg^{-1}, lithium–sulfur batteries represent a promising future energy storage device to power electric vehicles. However, the practical applications of lithium–sulfur batteries suffer from poor cycle life and low Coulombic efficiency, which is attributed, in part, to the polysulfide shuttle and Li dendrite formation. Suppressing Li dendrite growth, blocking the unfavorable reaction between soluble polysulfides and Li, and improving the safety of Li–S batteries have become very important for the development of high-performance lithium sulfur batteries. A comprehensive review of various strategies is presented for enhancing the stability of the anode of lithium sulfur batteries, including inserting an interlayer, modifying the separator and electrolytes, employing artificial protection layers, and alternative anodes to replace the Li metal anode.

1. Introduction

A rechargeable lithium–sulfur (Li–S) battery comprises a lithium metal anode and a sulfur cathode. It has a high theoretical specific energy (2600 Wh kg^{-1}), and a higher specific capacity (1675 mAh g^{-1}) based on the electrochemical reaction of $16Li + S_8 \rightarrow 8Li_2S$. Sulfur is environmentally friendly, low cost, and in natural abundance.[1] Li–S batteries are one of the most promising next-generation devices for high-energy-density storage, which is needed urgently to power electric vehicles. However, there are significant problems with Li–S rechargeable batteries which hinder their practical application, mainly their low S utilization and short cycling life. The poor electrical conductivity of elemental sulfur ($\approx 5 \times 10^{-30}$ S cm^{-1} at room temperature) is responsible for the low utilization of active materials and poor performance of Li–S batteries.[2] The dissolution of intermediate polysulfide products formed during the charge and discharge processes and the resulting shuttle phenomenon cause severe capacity fading and a lower Coulombic efficiency (**Figure 1**).[3] A large volume change (80%) between sulfur and Li_2S during the charge and discharge processes results in the structural collapse of the electrode and rapid capacity decay. Metallic Li anode forms mossy metal deposits and dendrite, causing low Coulombic efficiency, poor cycling life, and serious safety concerns.

Significant progress has been achieved recently in hindering the dissolution of polysulfides into electrolyte and improving the conductivity of sulfur by using various types of host cathode materials including carbonaceous nanomaterials (e.g., porous carbon, carbon nanotubes, carbon nanofibers and graphene), polymers and yolk-shell nanoarchitectures (e.g., sulfur–TiO_2 and sulfur–polyaniline), and optimizing the electrolyte composition, and configuring a new cell structure with polysulfide-blocking interlayers.[5,6] Although, these strategies can mitigate the shuttle effect of lithium polysulfides, and accommodate the volume expansion of sulfur, none of them has fully addressed the key challenges of Li–S batteries.

Lithium metal is an ideal anode material for the development of Li–S batteries with high energy densities because of its high theoretical capacity (3860 mAh g^{-1}), its light weight and electro-negative potential (−3.04 V versus standard hydrogen electrode).[7] However, during cycling, the corrosion reaction occurs and the formation of Li dendrites was found on the surface of lithium metal, leading to safety hazards, bad cycling stability and low Coulombic efficiency, crippling the commercialization of lithium–sulfur batteries (**Figure 2**).[8–10] A significant research effort has been devoted to resolving these problems.[11–13] Three strategies have been proposed: (i) designing novel cell configurations to mitigate the passivation of the lithium metal anode; (ii) introducing stable artificial interfaces to protect the lithium metal anode; and (iii) employing polymer and ceramic solid electrolytes to prevent dendrite penetration. Based on the developments made by these strategies, practical application and more improvements of Li–S batteries may be achieved by focusing on advanced anode designs.

In this review, we summarize the recent research progress made in the anode of Li–S batteries (**Figure 3**). Some effective strategies to protect the lithium metal anode will be discussed. The design, synthesis and characterization of other novel anodes of Li–S batteries will be also presented.

Dr. T. Tao, Prof. S. G. Lu, Prof. S. M. Huang
School of Materials and Energy
Guangdong University of Technology
Guangzhou 510006, P. R. China
E-mail: taotao@gdut.edu.cn
Dr. T. Tao, Y. Fan, Dr. W. W. Lei, Prof. Y. Chen
Institute for Frontier Materials
Deakin University
75 Pigdons Road, Waurn Ponds VIC 3216, Australia
E-mail: ian.chen@deakin.edu.au
Prof. S. M. Huang
Nanomaterials & Chemistry Key Laboratory
Wenzhou University
Wenzhou 325027, P. R. China

DOI: 10.1002/adma.201700542

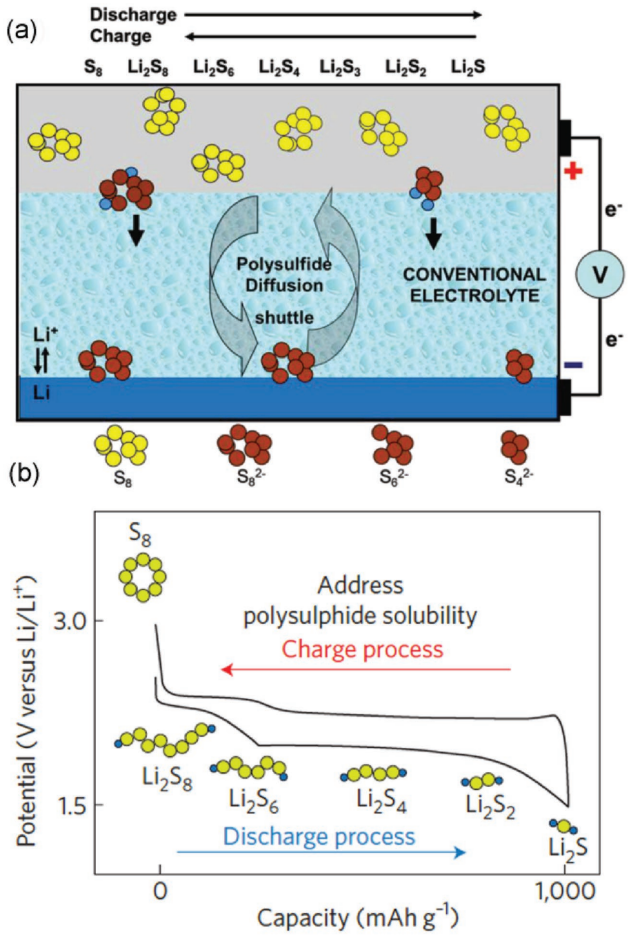

Figure 1. Schematic illustrations of a) shuttle effect and b) capacity fading of an Li–S battery. a) Reproduced with permission.[4] b) Reproduced with permission.[2] Copyright 2012, Nature Publishing Group.

2. Li Metal-Based Anodes in Li–S Batteries

As for lithium sulfur battery systems, the Li metal anode is highly reactive in the electrolyte and reacts easily with the shuttled soluble intermediate lithium polysulfides to form an unstable solid electrolyte interface (SEI) layer. The unstable SEI could not prevent the shape and volume changes of the lithium anode during cycling, leading to the dendritic growth of the Li metal. Furthermore, due to the breakdown of unstable SEI, the exposure of the fresh lithium surface to the electrolyte and parasitic reactions forming a new SEI layer, these decrease the efficiency of the lithium cycling. Therefore, the success of Li–S batteries depends on a reliable lithium metal anode. Many efforts have been made to improve the stability of the lithium-metal anode, such as designing novel cell configurations and introducing protective layers to the surface of the lithium anode. Recent key improvements are summarized below.

2.1. Interlayer Insertion

The insertion of a polysulfide-blocking interlayer between the Li anode and the S cathode has been demonstrated to be a

Tao Tao is an associate professor at the School of Materials and Energy, Guangdong University of Technology, China and an adjunct researcher at the Institute of Frontier Materials, Deakin University, Australia. He obtained his PhD degree in 2011 at the School of Chemistry and Chemical Engineering from Central South University, China and conducted three-year postdoctoral research at the Institute for Frontier Materials at the Deakin University. Australia. His current research focuses on the development of energy storage devices including lithium batteries and supercapacitors.

Shengguo Lu is currently a distinguished professor at the Guangdong University of Technology, and also a director of the Guangdong Provincial Research Center for Smart Materials and Energy Conversion Devices. Before joining the university, he was a senior research scientist consultant at the Strategic Polymer Sciences and an adjunct senior research associate at The Pennsylvania State University. His research interests include functional soft organic polymers, inorganic ceramics, organic–inorganic composites, and their applications as sensors, actuators, energy storages, and electrocaloric refrigerators.

Ying Chen is an Alfred Deakin Professor and the Chair in nanotechnology at Deakin University, Australia. He received his BSc from the Tsinghua University in China and PhD degree from University of Paris Sud, France. He has worked for 15 years at the Australian National University in Canberra and then joined Deakin University in 2009. His current research focuses on the synthesis of a variety of nanomaterials including boron nitride nanotubes and nanosheets, graphene and nanoparticles, and their applications in batteries, supercapacitors, environmental protection, and medical applications.

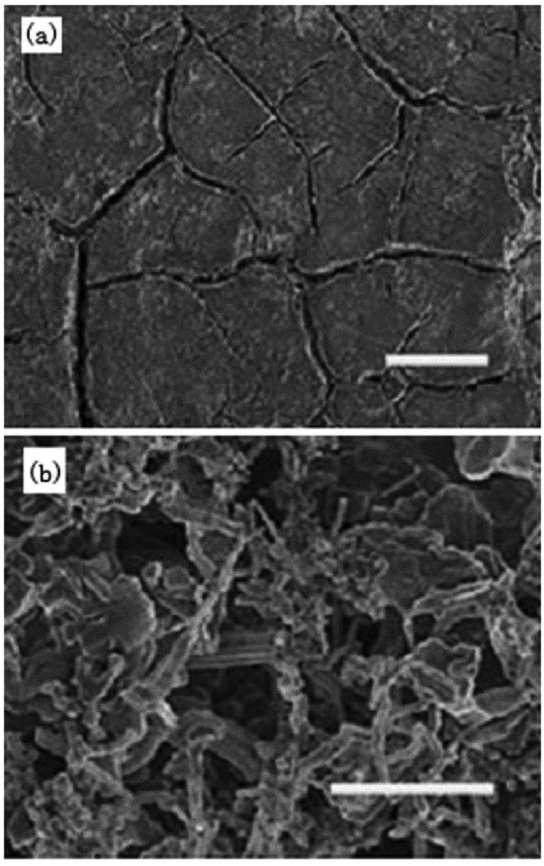

Figure 2. SEM images with different magnifications showing decomposed Li metal anode in an Li–S cell after 1000 cycles: a) low magnification and b) high magnification. Reproduced with permission.[29] Copyright 2014, Nature Publishing Group.

successful approach to significantly prevent the corrosion of the Li anode in an Li–S battery, including efficiently blocking the migration of polysulfides from the S cathode to the Li anode, thereby mitigating the passivation of Li anodes. A number of carbon-based interlayers have been found to improve the cycling stability of Li-S cells, including microporous carbon papers,[14] porous carbon nanofiber papers,[15] carbon fiber cloth,[16] N,S-codoped graphene (SNGE) films,[17] carbon nanofiber/polyvinylidene fluoride composite membranes,[18] TiO_2/graphene films,[19] conductive multiwalled carbon nanotube (MWCNT) films,[20,21] Fe_3C/carbon nanofiber webs,[22] Al_2O_3 coated nanoporous carbon cloth,[23] porous CoS_2/carbon papers[24] and graphene films[25] (**Figure 4**). It is believed that the thin interlayer of carbon materials can not only localize the soluble polysulfides and prevent the shuttle effect but also works as an upper current collector to improve the utilization of active material. Moreover, compared with pure carbon-based interlayers, carbon interlayers modified with metal compounds (e.g., TiO_2, Al_2O_3, CoS_2) or functionalized carbon interlayers more effectively confine the dissolved polysulfides. The carbon matrix adsorbs the polysulfides by the porosity of carbon materials, and the supported metal compounds or functional groups (e.g., nitrogen, sulfur) further capture the polysulfides by chemical combination.

As a model system, a full Li–S cell consisting of a pure sulfur powder cathode, a microporous carbon interlayer, a polypropylene separator, and a lithium foil was built with 1.85 M $LiCF_3SO_3$ and 0.1 M $LiNO_3$ in 1,2-dimethoxyethane(DME)/1,3-dioxolane (DOL) (1:1 v/v) as the electrolyte.[14] It was found that the conducting microporous carbon interlayer can reduce the surface resistance of the cathode, and the abundant micropores in the interlayer can effectively entrap the polysulfides. The cell with the microporous carbon interlayer delivers an excellent capacity above 1000 mAh g^{-1} at 100 cycles at a current density of 1675 mA g^{-1} within a voltage window of 1.5 and 2.8 V (vs Li^+/Li)

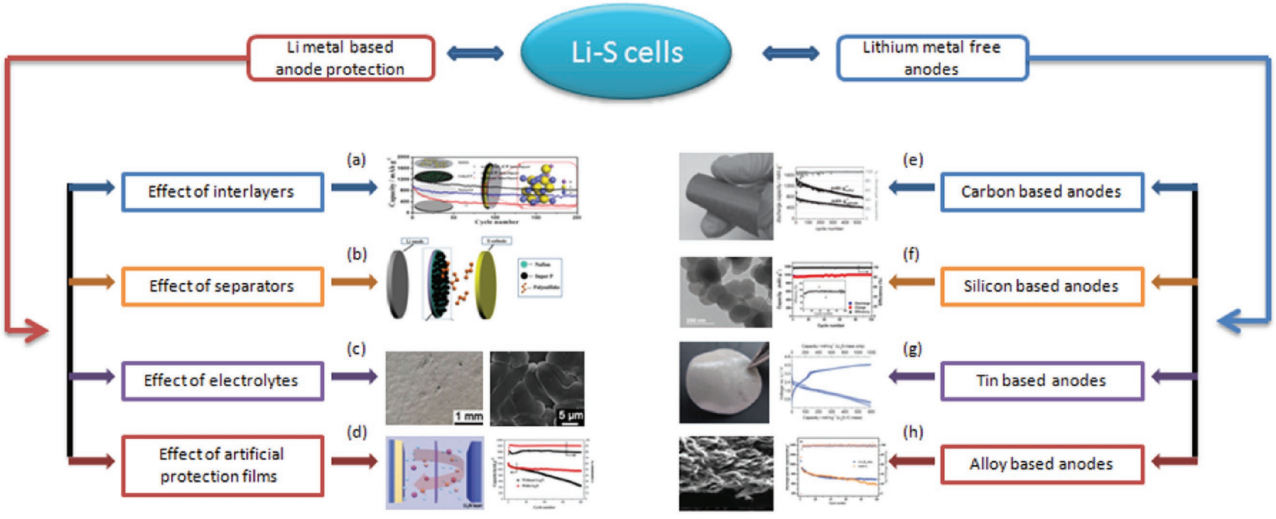

Figure 3. Selected effective strategies for improving the performance of the anodes for Li–S batteries: a) a hierarchically porous CoS_2/carbon paper interlayer, b) a facile and effective dual functional separator, c) addition of cesium ions (Cs^+) to the electrolyte, d) an Li_3N protection layer, e) a carbon based anode, f) a lithiated Si/SiO_x nanosphere anode, g) a polymer tin based anode, and h) an Li–B alloy anode. a) Reproduced with permission.[24] Copyright 2016, Elsevier. b) Reproduced with permission.[118] Copyright 2016, Elsevier. c) Reproduced with permission.[53] d) Reproduced with permission.[83] Copyright 2014, Royal Society of Chemistry. e) Reproduced with permission.[85] Copyright 2014, Wiley-VCH. f) Reproduced with permission.[95] Copyright 2015, American Chemical Society. g) Reproduced with permission.[97] h) Reproduced with permission.[100] Copyright 2014, Royal Society of Chemistry.

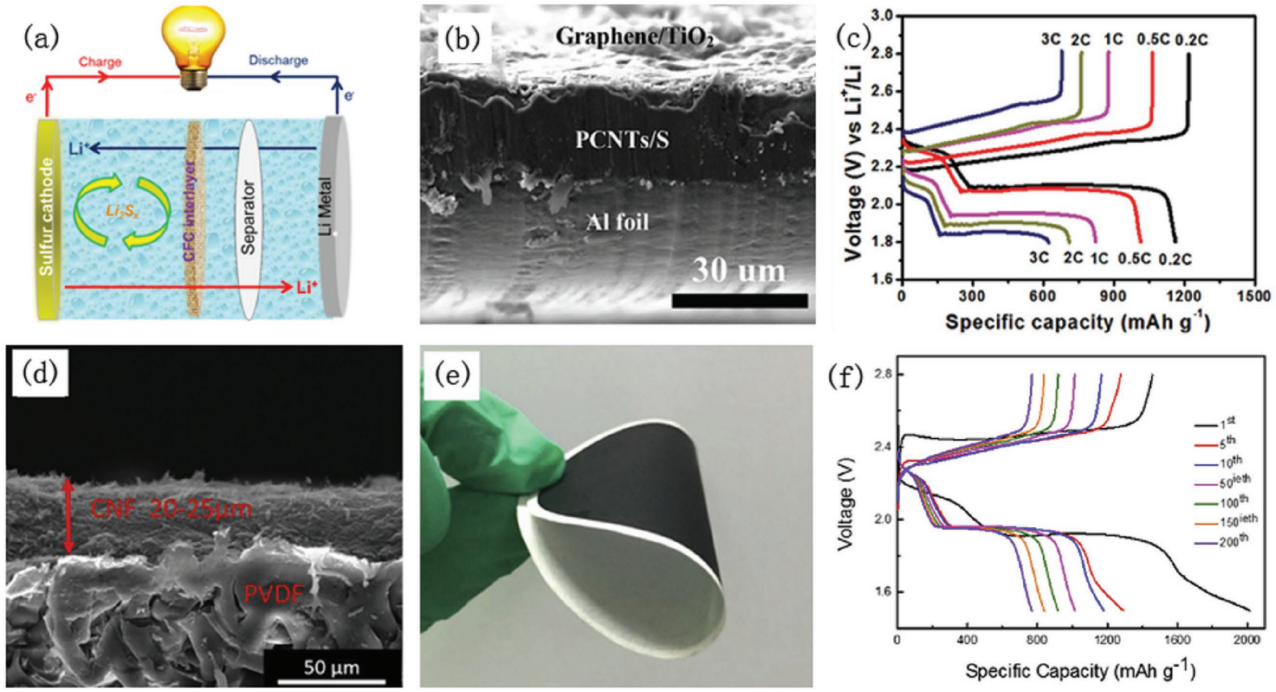

Figure 4. a) Schematic of the Li–S battery with a carbon based interlayer inserted between the electrode and the separator, b) typical SEM image of cross section of a fresh cathode with the graphene/TiO_2 interlayer, c) galvanostatic charge–discharge profiles of the cathode with the graphene/TiO_2 interlayer at various current rates, d) SEM image of the cross section of a carbon nanofiber/PVDF composite membrane, e) folded carbon nanofiber /PVDF composite membrane, and f) galvanostatic discharge/charge voltage profiles of an Li–S cell with a carbon nanofiber/PVDF interlayer at 0.5 C. a) Reproduced with permission.[16] Copyright 2016, Elsevier. b,c) Reproduced with permission.[19] Copyright 2015, Wiley-VCH. d–f) Reproduced with permission.[18] Copyright 2016, Elsevier.

and a high average Coulombic efficiency of 97.6%. In another case, a carbon fiber cloth interlayer with a high electric conductivity, a large surface area and excellent flexibility was directly inserted between a sulfur cathode and a separator to trap the soluble lithium polysulfide intermediates in an electrolyte of 0.4 M $LiNO_3$ additive and 1.0 M lithium bis(trifluoromethanesulfonyl) imide (LiTFSI) in DOL and DME (1:1 v/v).[16] A cell with this interlayer delivers a high reversible capacity (>560 mAh g^{-1}) at a large current density of 33.45 mA cm^{-2} over 1000 cycles between 2.8 and 1.6 V (vs Li^+/Li). A new design using a porous-CNT/S cathode coupled with a lightweight porous SNGE interlayer in an Li–S cell with an electrolyte of 1 M LiTFSI and 1% $LiNO_3$ in DOL/DME (1:1 v/v) was investigated (**Figure 5**).[17] The porous N, S-codoped graphene interlayer has excellent electric conductivity and can efficiently trap lithium polysulfides. The cell with this special interlayer can deliver a reversible specific capacity of ≈1460 mAh g^{-1} at 0.25 C (1C = 1675 mAg^{-1}) and shows a capacity degradation rate of 0.01% per cycle. These carbon-based interlayers show a significant effect in trapping lithium polysulfides and improving cycling life.

Conductive polymer interlayers were also developed to mitigate the shuttle effect and to protect the Li anode to improve the cycling stability of the Li–S batteries (**Figure 6**a). Conductive polymer, including polyaniline, polypyrrole, and polythiophene, lower the charge transfer resistance of electrodes and suppress lithium polysulfides in the cell due to their high electrical and ionical conductivity, and the H-bonds between the protondoped polymers and lithium polysulfides. Polypyrrole-based interlayers between the Li anode and the S cathode have been fabricated to enhance the cycle performance of the Li–S battery.[26,27] The polypyrrole functional interlayer could mitigate the dissolution and migration of lithium polysulfides in the electrolyte, and prevent the corrosion of the Li anode during the charge and discharge process because of the H-bond and high specific surface areas. The Li–S cell containing the polypyrrole nanotube interlayer and an electrolyte consisted of 1 M LiTFSI in DOL and DME (1:1 v/v) with no $LiNO_3$ additive exhibits a high specific capacity (>1100 mAh g^{-1}), good cycle stability (>700 mAh g^{-1} over 300 cycles) and high Coulombic efficiency (about 92%) in a voltage range of 2.8–1.8 V (vs Li/Li^+).[27] A nano-Li^+-channel interlayer of the Li–S battery was synthesized by swelling the dense polyvinylidene fluoride (PVDF) membrane in an electrolyte containing 1 M LiTFSI in DOL and DME (1:1 v/v) without $LiNO_3$ additive, and its special ions transport channels could selectively separate the Li^+ and polysulfide.[28] Consequently, the nano-Li^+-channel interlayer can confine the lithium polysulfide shuttling, leading to a high specific capacity as well as a good cyclability between 1.5 and 2.8V.

Besides the above-mentioned interlayers between the cathode and the separator, a hybrid anode composed of an electrically connected graphite interlayer and Li metal was proposed as a new design of the Li–S batteries to address the problems of lithium polysulfides shuttle and lithium dendrite (Figure 6b).[29] In this design, the separator is placed between the Li metal and the graphite film to form the anode, and the graphite film electrically connected with the Li metal. The lithiated graphite acts as an artificial solid-state electrolyte interface to help supply Li^+

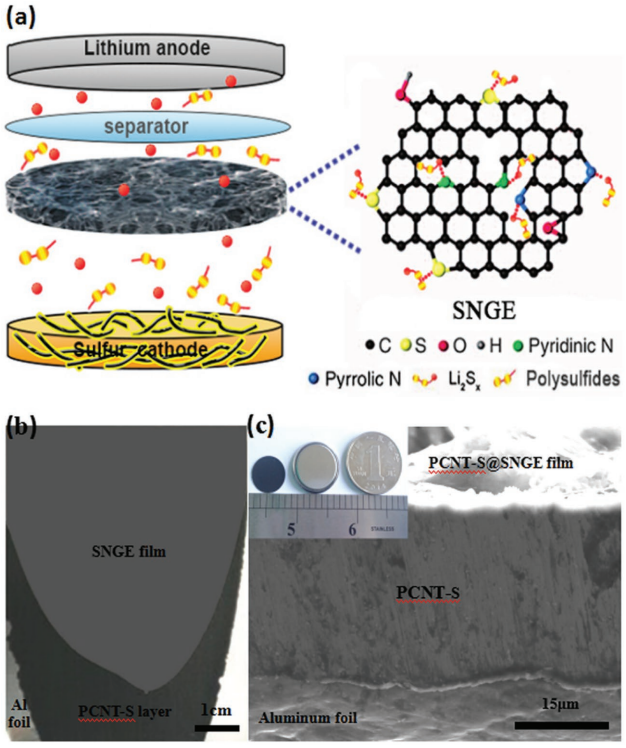

Figure 5. a) Schematic of electrode configuration of an Li–S battery with an SNGE interlayer, b) Photograph and c) cross-sectional SEM image of the cathode with an SNGE interlayer, and inset are photographs of the PCNT-S@SNGE cathode and the as-made Li–S cell. Reproduced with permission.[17] Copyright 2016, Royal Society of Chemistry.

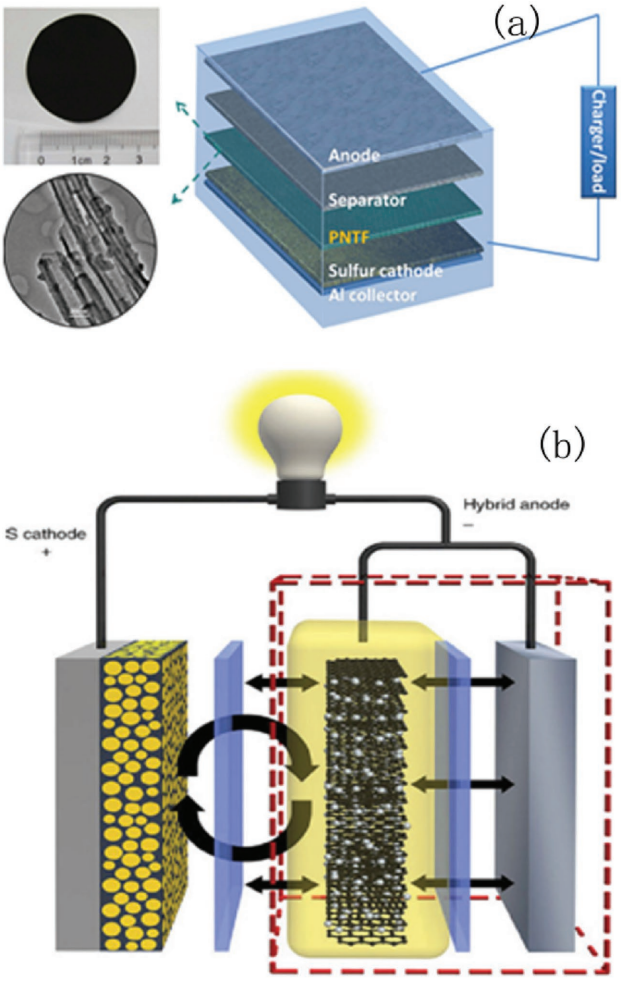

Figure 6. a) Schematic cell configuration of rechargeable Li–S batteries with a polypyrrole nanotube film, and b) hybrid anode design. a) Reproduced with permission.[27] Copyright 2015, Elsevier. b) Reproduced with permission.[29] Copyright 2014, Nature Publishing Group.

ions on demand and minimize deleterious parasitic reactions between the lithium polysulfides and Li metal surface. The Li–S cell incorporating the hybrid anodes with an electrolyte of 0.1 M $LiNO_3$ and 1 M LiTFSI in DOL/DME (1:1 v/v) delivers capacities up to 800 mAh g^{-1} over 400 cycles at a high rate of 1737 mA g^{-1} between 1.0 and 3.0 V.

The interlayer insertion between the separator and sulfur electrode has been proven to be an effective strategy to stabilize the lithium anode morphology and fabricate high-performance Li–S batteries. These interlayers with porous, conductive and flexible structures could serve as a barrier to improve the active material utilization, regulate polysulfide shuttle, and maintain cycle stability and good efficiency. A porous structure is crtitical for absorbing the polysulfides, high electrical conductivity facilitates faster electron transfer, and the flexible structure is useful in reducing the volume change of the cathode. In further studies, the thickness/weight of the applied interlayers should be reduced as much as possible. Novel interlayers with proper pore structure, excellent mechanical stability and conductive property need to be developed. Insertion of interlayers between the separator and anode might be needed for next generation Li–S batteries.

2.2. Separator Modification

The separator, a nanoporous polymer membrane, is a basic component in an Li–S battery, and functions as an ion conductor to maintain the pathway and an electron insulator to prevent short circuit. Polysulfides produced during the discharge and charge processes can diffuse freely through the separator and react with the Li anode, and cause the degradation of the Li anode. Therefore, the modification of separators has been proposed to inhibit the polysulfide shuttling in organic electrolytes and also protect Li anodes. A number of functional layers, including carbons, polymers, oxides, and their composites, have been developed to modify the separator for trapping the soluble polysulfides in electrolyte. These modified separators have exhibited great success in improving the performance of Li–S batteries.

Again, carbon material is the most popular material for modifying the separators of the lithium–sulfur batteries (**Figure 7**),[30] because it has the following advantages: (i) a high electrical conductivity for providing a fast and short-distance electron transport; and (ii) a porous structure, large conductive surface area or sufficient pathways to absorb the dissolved polysulfides and regulate the polysulfides shuttle. Various carbon materials such as carbon nanotubes,[31] graphene,[32,33] carbon

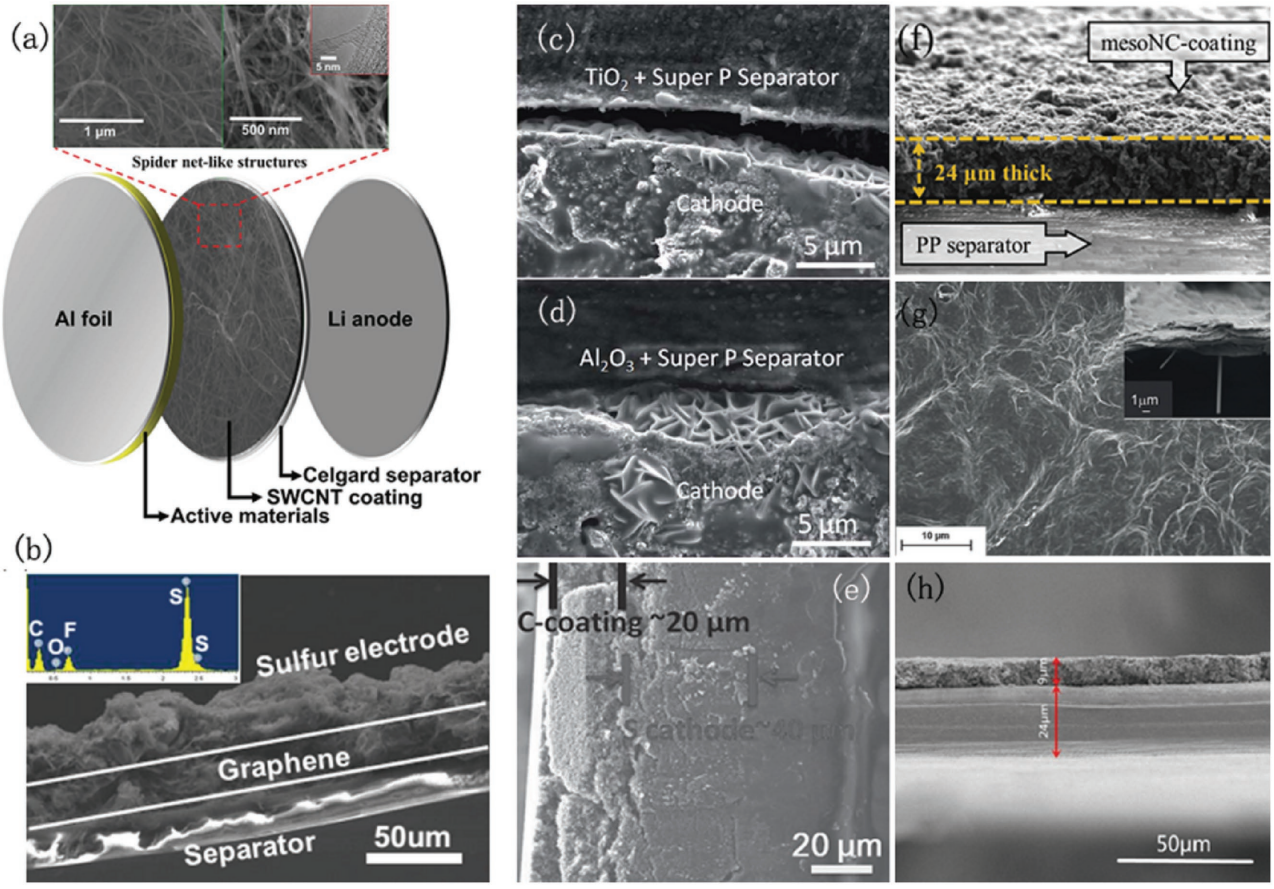

Figure 7. a) Schematic and SEM images of the single-wall carbon nanotube modulated separator configuration. Cross-section SEM images of various samples: b) Integrated sulfur electrode with the G@PP separator and corresponding EDS spectrum, c,d) TiO_2–Super P coated separator–cathode interface and the Al_2O_3–Super P coated separator–cathode interface, e) cell with the C-coated separator, f) N-doped mesoporous carbon-coated separator, g) fluoro-functionalized reduced graphene oxide separator, and h) N-doped porous carbon nanowire-modified separator. a) Reproduced with permission.[31] b) Reproduced with permission.[32] c,d) Reproduced with permission.[30] Copyright 2014, Royal Society of Chemistry. e) Reproduced with permission.[34] f) Reproduced with permission.[35] Copyright 2016, Elsevier. g) Reproduced with permission.[33] h) Reproduced with permission.[36] Copyright 2016, Elsevier.

black,[34] nitrogen-doped mesoporous carbon,[35] and N-doped porous carbon nanowires[36] have been tried. For example, the single-wall carbon nanotube modified separator has been developed to reduce the fast polysulfide migration and prevent the Li anode degradation in the Li–S cell with an electrolyte comprising 0.1 M $LiNO_3$ and 1.85 M $LiCF_3SO_3$ in DOL/DME (1:1 v/v).[31] The separator was prepared by vacuum filtering a solution of isopropyl alcohol and single-wall carbon nanotube (0.04 mg mL^{-1}) on a Celgard 2500 separator. The carbon coating layer with good electrical conductivity also serves as an upper-current collector to repeatedly use the trapped active materials during cycling. A cell employing the single-wall carbon nanotube coated separator shows a high reversible capacity of above 501 mAh g^{-1} at 0.2 C between 1.8 and 2.8 V after 300 cycles. The fluoro-functionalized reduced graphene oxides with hydrophobic properties can be directly used as an effective separator for Li–S cells with an electrolyte (1 M LiTFSI in sulfolane, 60 mL mg^{-1} of sulfur).[33] It is found that the separator of fluoro-functionalized reduced graphene oxides with a thickness of 1–2 mm decreases polysulfide concentration and the homogenous distribution of end-discharge products during cycling at 0.1 C between 3.0 and 1.5 V. A simple modification of the commercial polypropylene separator with a thin layer of melamine-derived N-doped mesoporous carbon was proposed to promote the interfacial interaction between the dissolved polysulfides and the N-dopants on carbon-coating by coupling interactions.[36] It was fabricated by a slurry coating method (0.4 mg cm^{-2} in weight), and 1 wt% $LiNO_3$ and 1.0 M LiTFSI in DOL/DME (1:1 v/v) used as an electrolyte. The unique physical and interfacial chemical properties of such carbon coating layer are effective in protecting the Li anode and improve the cycling stability of 0.08% capacity fading per cycle at 0.5 C between 1.7 and 2.8 V.

Polymer modified separators, including an ion selective Nafion membrane layer,[37] a mixture of Nafion and super P,[38] and a polydopamine layer,[39] have been demonstrated to effectively block the transportation pathway of the dissolved polysulfides and maintain the stability of the electrode structure (**Figure 8**). The polymer modified functional separators can confine polysulfide anions to the sulfur cathode side and prevent them from diffusing to the lithium anode side. Also, a Nafion film coated on the Celgard 2400 membrane was

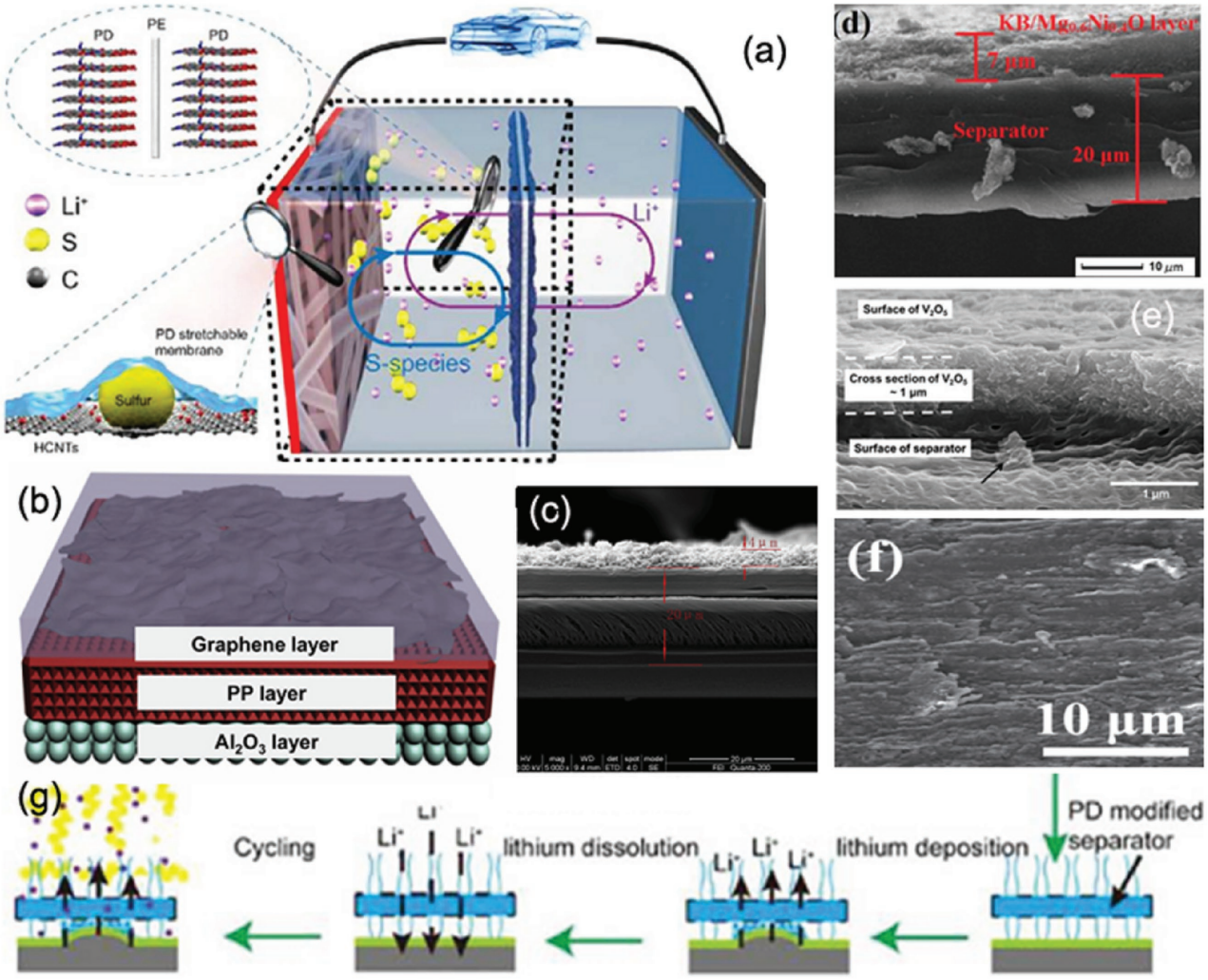

Figure 8. a) Schematic of the Li–S battery with the polydopamine coated separator and g) Li anode structure using the polydopamine coated separator, b) schematic illustration of the structure of a trilayer graphene-polypropylene-Al_2O_3 separator, c) SEM image of the Al_2O_3-coated PP/PE/PP separator. d) SEM image of the surface of Ketjen Black/$Mg_{0.6}Ni_{0.4}O$ composite coated separator after 100 cycles, e) cross-sectional SEM images of V_2O_5 layer on polymeric battery separator, and f) surface SEM image of Li anode with glass fiber separator after 100 cycling. a,g) Reproduced with permission.[39] Copyright 2014, American Chemical Society. b) Reproduced with permission.[44] Copyright 2016, Elsevier. c) Reproduced with permission.[40] Copyright 2014, Elsevier. d) Reproduced with permission.[43] Copyright 2017, Elsevier. e) Reproduced with permission.[41] Copyright 2014, American Chemical Society. f) Reproduced with permission.[47] Copyright 2016, Elsevier.

employed as an ion selective membrane to effectively block the shuttle of polysulfides and allow the free transportation of lithium cations.[37] The ion selective membrane acts as an electrostatic shield for polysulfide anions in the Li–S cell, and the diffusion of polysulfide is localized on the cathode side, leading to a small cycle decay of 0.08% per cycle for 500 cycles at 1C in a voltage range of 2.8–1.7 V. The polydopamine modified cathode and separator have been developed to suppress polysulfide transportation and improve the performance of the Li–S battery.[39] The bilaterally polydopamine separator was synthesized by a modified polydopamine in situ coating process. It is believed that the polydopamine can induce agglomerate nucleation to form many petals, and bind these petals together with its adhesive properties, decreasing charge transfer resistance and SEI resistance for improved cycle performance. The cell achieves a capacity fade of only 0.018% per cycle and about 99% Coulombic efficiency at a current density of 3350 mA g^{-1} over 3000 cycles.

Functional separators were also modified with metal oxides and their composites to improve the electrochemical performance of the Li–S batteries, such as Al_2O_3,[40] V_2O_5,[41] MnO/Ketjen Black,[42] and $Mg_{0.6}Ni_{0.4}O$/Ketjen Black composite,[43] because their strong polysulfide binding effects of oxygen-rich metal oxides help to suppress the diffusion of polysulfides to the lithium anode side. To further address the shuttle effect of lithium polysulfides and the corrosion problem of Li anodes, multimodified separators have been prepared, including three-layer separators of carbon nanotube/polypropylene/Al_2O_3,[44] carbon/lithium aluminum germanium phosphate/Celgard,[45] and sulfur/graphene/polypropylene.[46] The graphene/polypropylene/Al_2O_3 separator,[44] prepared by a blade coating process, shows a dual function. Graphene coated

on one side of the polypropylene separator (a thickness of 3–5 mm, 0.10 mg cm^{-2}) serves as an electrolyte reservoir and a conductive layer to allow for rapid ion and electron transport; the safety and thermal stability of the cell can be further enhanced by the Al_2O_3 particles coated on the other side (a thickness of 5 µm, 1.22 mg cm^{-2}). This cell delivers a remarkable reversible capacity of 804.4 mAh g^{-1} (75% capacity retention) at 0.2 C after 100 cycles.

The recent progress in novel separators opens up a different direction toward high-performance Li–S cells. A porous glass fiber membrane with superior thermal stability and excellent electrolyte wettability has been evaluated as a potential separator for Li–S batteries.[47] The porous glass fiber membrane was synthesized from borosilicate microfibers and could reduce the rapid diffusion of polysulfides to the Li anode side, and enhance its electrochemical performance (a capacity of 617 mAh g^{-1} at 0.2 C over 100 cycles). A metal-organic framework-based separator, $Cu_3(BTC)_2$/ graphene oxide separator, was fabricated by adhering the adjacent $Cu_3(BTC)_2$ and graphene oxide layers to the filter membrane two or three times. The separator could efficiently sieve Li^+ ions while blocking undesired polysulfides migrating to the anode.[48] The cell with this separator shows an amazing capacity of 855 mAh g^{-1} at 1 C after 1500 cycles between 1.5 and 3.0 V. A promising approach has been proposed to enhance the cycling stability of Li metal anode by using a facile coating of commercial separator (Celgard 2325) with thermally conductive BN nanosheets.[49] The separator was made by coating one side of the Celgard 2325 separator with a BN/PVDF/NMP suspension. The BN-coating on the polypropylene/polyethylene separator shows a high thermal conductivity of 82 W mK^{-1}. The cell using this separator can maintain a high Coulombic efficiency of 92% after 100 cycles at 0.5 mA cm^{-2} in a common $LiPF_6$—ethylene carbonate (EC)—diethyl carbonate (DEC) electrolyte.

The mechanism of modified separators is similar to that of interlayers, focusing on the inhibition of polysulfide diffusion and improvement of the lithium anode lifespan. More efforts on new generation multifunctional separators, such as the hybrid modification and composite of separators, are greatly required. Also, developing the advanced separator and interlayer combination systems will bring new opportunities into this field in the future.

2.3. Electrolyte Additives

The electrolytes are important in the development of high-performance Li–S batteries because their composition and type strongly affect the polysulfide distribution in the cell. The chemical composition and microstructure of the passivation layer on the lithium surface is also related to the electrolytes used. Several special electrolytes, e.g., organic liquid electrolytes, ionic liquids electrolytes, and polymer and solid electrolytes, have been developed to control dendrite formation and the polysulfide shuttle of Li–S batteries.

The most common Li–S liquid organic electrolytes contain lithium salts such as lithium bis(trifluoromethanesulfonyl) imide ($Li[N(SO_2CF_3)_2]$ or Li(TFSI), $Li[SO_3CF_3]$), and $LiClO_4$, and a mixture of organic solvents including DOL, DME, tetraethylene glycol dimethyl ether (TEGDME), fluoroethylene carbonate and tetrahydrofuran.[50] Dissolution of lithium polysulfides is inevitable in these liquid electrolytes, resulting in the shuttle effect and dendrite formation on the metallic Li anode surface. Additives have been developed to reduce the dissolution of polysulfides in the liquid electrolytes (**Figure 9**). A successful example in this area is that lithium nitrate ($LiNO_3$) is a powerful electrolyte additive.[51–53] It is found that $LiNO_3$ can contribute to an increase of the ionic conductivity for the electrolyte, from 0.8 to 1.4 mS cm^{-1}.[54] It is the critical component to form a protective surface film of lithium anode, and acts as an oxidizing agent. The reduced Li_xNO_y species, together with the oxidized polysulfides and Li_xSO_y moieties, could enhance the passivation of the Li anodes and alleviate parasitic reactions between lithium metal and polysulfide species. Lithium bisoxalatoborate (LiBOB),[55] copper acetate ($Cu(OOCCH_3)_2$),[56] lithium oxalyldifluoroborate (LiODFB),[57] and phosphorus pentasulfide (P_2S_5)[58] have also been used as electrolyte additives to promote the formation of a surface passivation layer on the lithium electrode. The stable lithium–metal surface and the high Li–S battery's performance are obtained in the presence of LiBOB, $Cu(OOCCH_3)_2$, LiODFB, or P_2S_5 in the electrolytes. Additionally, the low conductivity and high viscosity of concentrated electrolytes with less free solvent molecules could effectively inhibit polysulfide dissolution, diminish the side reactions between the Li metal and the polysulfide species, protect the Li anode, and suppress Li dendrite formation.[59]

In another direction, researchers have examined the possibilities of using ionic liquid electrolyte or polymer/solid-state electrolyte to reduce the dissolution and shuttle of polysulfides. Ionic liquids with high electrochemical stability, wide potential window and low vapor pressure are regarded as a new class of electrolyte materials for Li–S batteries because they can provide low solvation power toward polysulfides and reduce the shuttle effect (**Figure 10**).[60,61] A series of ionic liquid electrolytes, including $Pyr_{1,201}$TFSI (*N*-methoxyethyl-*N*-methylpyrrolidinium bis-(trifluoromethanesulfonyl)-imide)/TEGDME electrolyte with Lithium difluoro(oxalate)borate (LiDFOB)/ LiTFSI binary lithium salts,[62] a hybrid electrolyte of N-methyl-N-butylpyrrolidinium bis(triuoromethylsulfonyl)imide (Py_{14}TFSI) and LiTFSI dissolved in a mixture of DOL and DME,[63] and LiTFSI-$Pyr_{1,201}$TFSI/TEGDME/ LiTFSI,[64] have been prepared to promote the formation of an SEI layer on the surface of an Li anode during charge and discharge cycling. A smooth surface morphology of Li anode covered in a compact and uniform film was observed during cycling in this ionic liquid electrolyte. For example, it has been demonstrated that a Py_{14}TFSI additive could enhance the thermal stability and lower the flammability of electrodes.[63] The conventional electrolyte incorporated with the high viscosity ionic liquid Py_{14}TFSI contributes to the formation of a more stable and higher quality SEI layer on the Li metal surface to protect the Li anode.[65] The TFSI anion could maintain stable charge and discharge, and the ether group in the cation of the ionic liquid effectively improves the conductivity of electrolytes. The effect of both ionic liquid 1-butyl-1-methylpyrrolidinium bis(trifluoromethanesulfonyl) imide (C_4mpyr-TFSI) and $LiNO_3$ to stabilize lithium metal surfaces in Li–S batteries was also investigated.[66] The passivation film modified by the resultant S_xO_y could protect the Li anode from

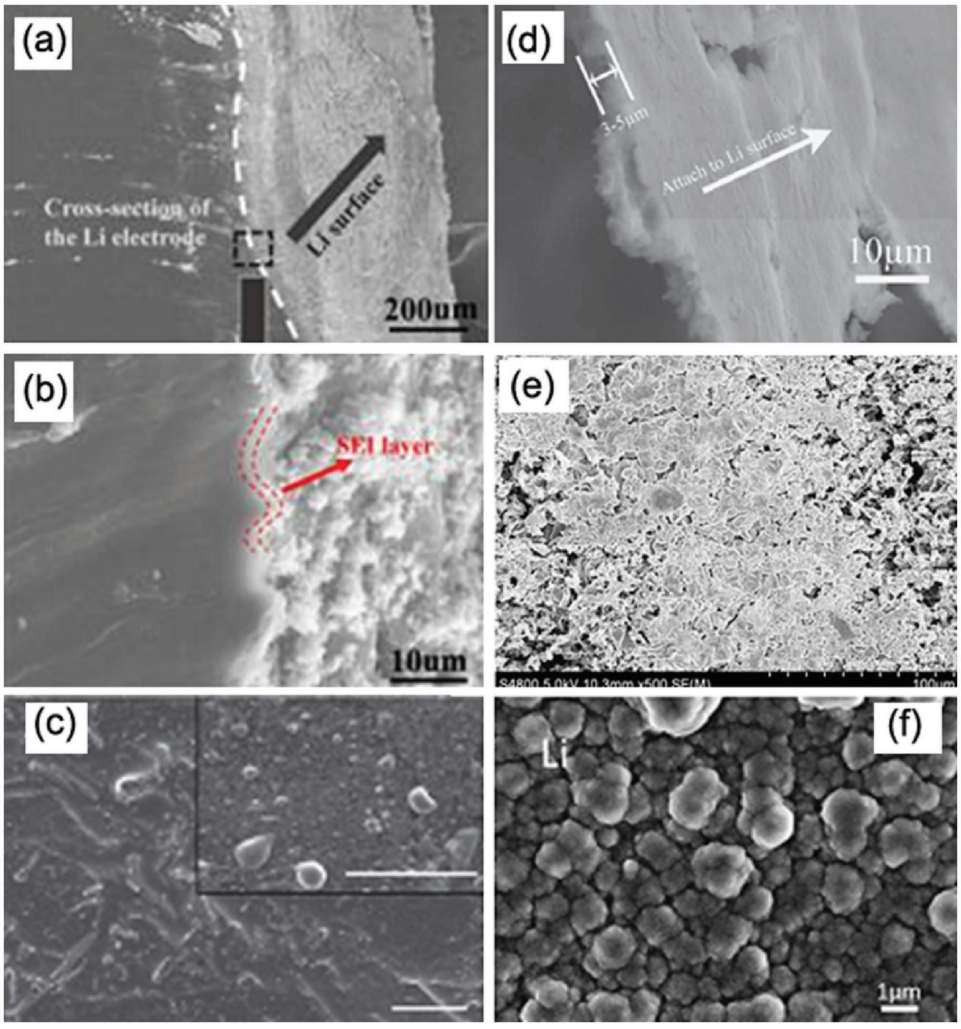

Figure 9. SEM images of the cross section of the lithium electrode: a) low and b) high magnifications with 2% LiODFB after 50 cycles, c) using the $LiPF_6/[C_3mPyr^+][FSI^-]$ electrolyte after 12 d, d) cycled with P_2S_5 in the electrolyte, e) with 10 wt% LiBOB additive after 50 cycles, and f) with 5 M LiFSI/DM after 150 cycles. a,b) Reproduced with permission.[57] Copyright 2014, American Chemical Society. c) Reproduced with permission.[119] Copyright 2016, Nature Publishing Group. d) Reproduced with permission.[58] e) Reproduced with permission.[55] Copyright 2012, Springer. f) Reproduced with permission.[59]

direct corrosion reactions with polysulfides. More reversible redox reactions induced by ionic liquid in the battery and consequent high capacity retention of above 99% over 100 cycles is obtained.

Gel polymer and solid-state electrolytes could be more effective than a liquid electrolyte in terms of reducing the dissolution and shuttle of polysulfides, and minimizing the safety concern associated with the liquid electrolyte. Generally, the application of Li–S batteries with polymer electrolytes suffers from a low ionic conductivity at room temperatures.[67] Several polymer architectures have been developed to enhance the ionic conductivities and mechanical properties of polymer electrolytes. For example, a pentaerythritol tetraacrylate (PETEA)-based gel polymer electrolyte with an extremely high ionic conductivity (1.13×10^{-2} S cm^{-1}) was reported (**Figure 11**).[68] The polysulfides immobilized by PETEA-based gel polymer electrolyte and the formation of a stable passivation layer on the sulfur electrode surface induced by the polymer matrix of GPE result in the improved performance of Li–S batteries. Poly(ethylene oxide) (PEO)-based polymer electrolytes with lithium salts containing finely dispersed nanosized ceramic fillers including ZrO_2,[69] Al_2O_3,[70] and SiO_2[71] have also been developed. These electrolytes exhibit excellent thermal stability, good interfacial stability, and high ionic conductivity. Various other solid electrolytes with high ionic conductivity at room temperature, such as $Li_{3.25}–Ge_{0.25}P_{0.75}S_4$,[72,73] $Li_2S–P_2S_5$,[74–76] $Li_{10}GeP_2S$,[77] $Li_2S–GeS_2–P_2S_5$,[78] and $Li_2S–P_2S_5$/hydroxyterminated perfluoropolyether (PFPE-diol)/(LiTFSI),[79] have been investigated for Li–S batteries. Although, the solid electrolytes could effectively eliminate the polysulfide dissolution problem, the major challenges remain the realization of smooth electrode/electrolyte interfaces and the decrease in large interfacial impedance between the resultant solid state electrolyte and the solid electrode in Li–S batteries. Furthermore, few reports directly indicate that solid-state electrolytes could prevent Li dendrite in Li–S batteries. Further work should focus on these issues in future.

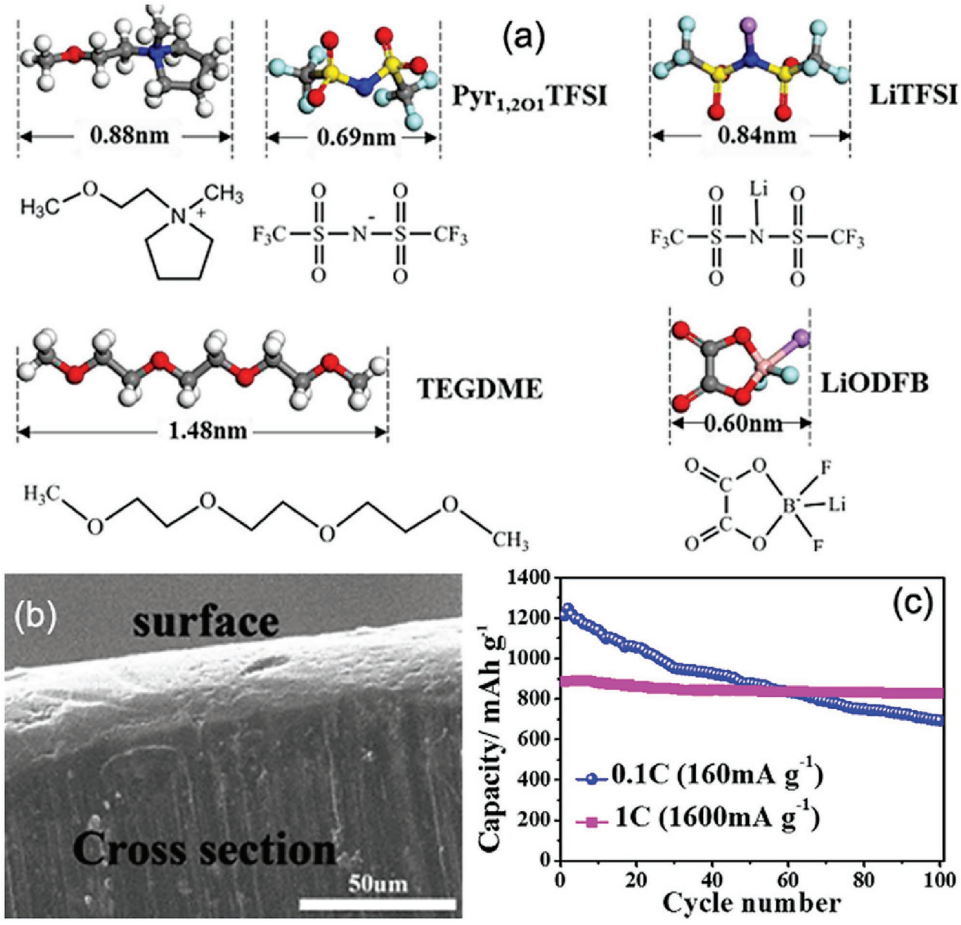

Figure 10. a) Molecular structures and sizes of the electrolyte components: $Pyr_{1,2O1}TFSI$, TEGDME, LiTFSI, and LiODFB. b) Cross-section SEM image of lithium metal cycled in 50% I L containing electrolyte for 100 cycles at 0.2 C. c) Cycling performance of the Li–S batteries with the LiTFSI-$P_{1,2O1}TFSI$/(30 wt%)TEGDME electrolyte. a) Reproduced with permission.[62] Copyright 2015, Elsevier. b) Reproduced with permission.[63] Copyright 2013, Royal Society of Chemistry. c) Reproduced with permission.[64] Copyright 2015, Elsevier.

Electrolyte optimization, as one of the most important solutions, is believed to improve the cycling performance and safety of practical Li–S cells. The possibility of changing electrolyte properties, including viscosity and conductivity, is increasing to fully meet the new requirements of different Li–S battery concepts. Organic liquid electrolytes including 1 M LiTFSI 1,3-dioxane (DIOX): DME (1:1 v/v) (+$LiNO_3$) are indeed very valid for balancing the requirements of Li–S batteries.

Most of the ionic liquid electrolytes investigated show excellent electrochemical performance. Novel electrolytes and additives for Li–S batteries could be effective in promoting Li–S battery performance. The polymer and solid electrolytes could also be promising alternatives to solve the problem of the soluble polysulfides shuttle. However, understanding the electrochemical mechanisms involved in various electrolyte systems for Li–S batteries is still a big challenge because of their complexity.

2.4. Artificial Protection Films

As an alternative to protect SEI layers in situ formed on the interface between the Li anode and the electrolyte, thin artificial films have been employed to protect the Li anode during the charge and discharge process (**Figure 12**). The cell uses a thin Li–Al alloy layer coated Li anode and shows better electrochemical performance than the Li–S cell with pure Li anode between 3.0 and 1.2 V at 0.2 C in an electrolyte (3 M LiTFSI in DME:DIOX (1:1, v:v)).[80] The Li-Al alloy layer is laminated on the Li surface at 90 °C for 24 h under pressure to stabilize polarization during plating and deplating of Li ions, and mitigates the polysulfide shuttle phenomenon. The effects of the composite protective film of Li–Al alloy and lithium pyrrolide on the electrochemical performance of the Li anode in a nonaqueous 1 M $LiPF_6$/EC + DMC electrolyte were also investigated.[81] Both $AlCl_3$ and pyrrole were simultaneously added to the nonaqueous electrolyte to prepare the protective film. The Li anode with the composite protective film shows higher stability and better electrochemical properties than that with the single protective film (Li–Al alloy layer or lithium pyrrolide film). The polymer-based protective film on the surface of the Li anode was prepared by UV curing,[82] and the film can reduce the growth of the SEI layer and suppress the reaction between the Li and soluble polysulfides to enhance the charge and discharge performance

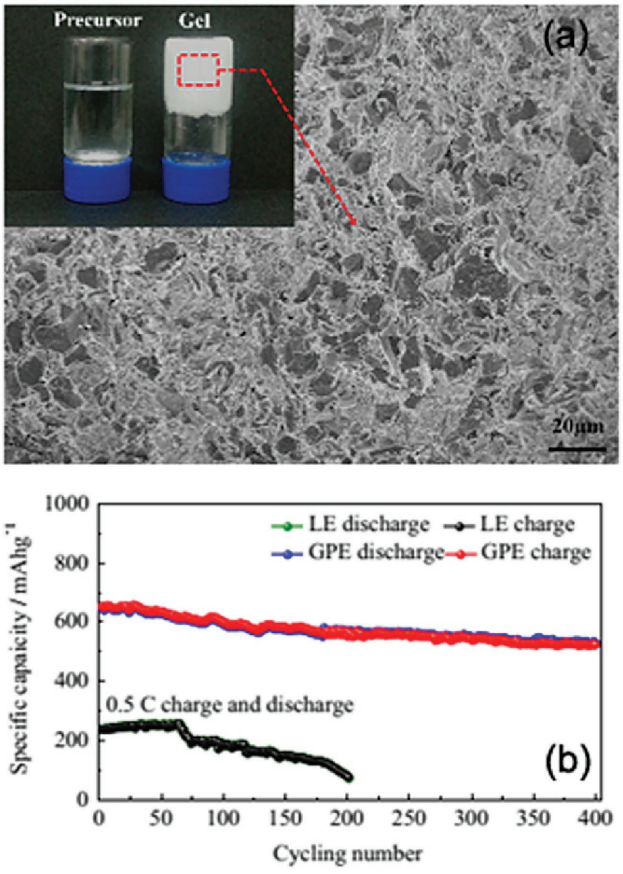

Figure 11. a) SEM image of the pentaerythritol tetraacrylate-based gel polymer electrolyte, and b) cycling performances of the S/liquid electrolyte/Li cell and S/gel polymer electrolyte /Li cell at 0.5 C. Reproduced with permission.[68] Copyright 2016, Elsevier.

of Li–S batteries. The unit cell was assembled by stacking a plasticized polymer electrolyte between the sulfur cathode and lithium anode with an aluminized polyethylene bag (the size of 2 cm × 2 cm). In order to further improve the cycle performance of Li–S batteries, the surface of the Li anode was in situ coated with an Li_3N protective layer (200–300 nm) via the direct reaction between the Li and N_2 gas at room temperature.[83] The Li_3N layer has a high ionic conductivity which benefits the migration of Li^+ and prevents the Li dendrites originating from a nonuniform deposition of Li. The Li–S battery with an Li_3N layer coated Li anode delivers the discharge capacity of 773 mAh g^{-1} after 500 cycles with an average Coulombic efficiency of 92.3% at 0.5 C between 1.8–2.6 V in an electrolyte (1 M LiTFSI $LiNO_3$ in DOL/DME (1:1 v/v))without $LiNO_3$.

The above-mentioned thin artificial protective layer is the closest layer to the Li anode, which effectively prevents side reactions between polysulfide and lithium. The thin artificial protective layer should have high conductivity, chemical stability and ionic selectivity. Further effort is required to develop the new artificial protective layers via a simple synthesis procedure and at low cost.

3. Lithium Metal-Free Anodes in Li–S Batteries

Full battery cells, based on sulfur or Li_2S cathodes and metal-free anodes such as carbon, silicon, tin, and alloy, have attracted great attention in the field of Li–S batteries in recent years due to their low weight, high conductivity, large theoretical specific energy, and theoretical volumetric energy density. Most of the metal-free anodes should be prelithiated versus lithium metal before they are assembled in the full Li–S cell. Although the metal-free system can effectively avoid the safety issues and decrease Li excess associated with the use of an Li anode in conventional batteries, the low capacity of these anodes in accommodating Li ions could compromise the overall energy density of Li–S batteries.

A full Li–S battery using a graphite-based anode and sulfur–carbon cathode was developed recently.[84] The anode was prelithiated by contact with a lithium foil in 1 M $LiPF_6$ EC:DMC (1:1, v:v). It delivers a reversible capacity of 500 mAh g^{-1} at 1C, and shows a high Coulombic efficiency and limited polarization. A hard carbon has been used as an alternative anode in an Li–S cell.[85] A specific capacity of up to 753 mAh g^{-1}, and a high Coulombic efficiency of about 99% over 550 cycles, are achieved at a current rate of 334 mA g^{-1} between 2.6 and 1.0 V. A Li_2S-graphite full cell exhibits a reversible capacity of about 600 mAh g^{-1} after 150 cycles at 0.1 C between 0.5 and 3.0 V, and the electrode was prelithiated by a sprinkling process with a metal lithium powder.[86] A cell with a sulfur cathode and lithiated graphite anode was investigated, and the graphite anode was prelithiated by fabricating a half cell (Li/graphite). The final cell shows a reversible capacity of 515 mAh g^{-1} over 50 cycles at 0.2 C between 1.7 and 3.0 V.[87] An advanced lithium metal-free cell based on a lithiated carbon-silicon nanocomposite anode combined with a sulfur–carbon composite cathode, separated by a glycol-based electrolyte, was proposed.[88] The carbon-silicon nanocomposite was prelithiated by directly pressing it on a lithium foil in an electrolyte (1.2 M $LiPF_6$ EC:EMC, weight ratio of 3:7) for 12 h. This full cell delivers a specific capacity of 300 mAh g^{-1} at a current rate of 0.5 A g^{-1} between 1.25 and 2.8 V after 50 cycles in an electrolyte ($LiCF_3SO_3$/TEGDME, a molar ratio of 1:4).

Besides the carbon-based anodes, Si-based anodes have been proposed to address the safety issues of Li–S batteries. Although Si-based anodes are regarded as the most interesting alternative to metallic lithium, because of their highest theoretical gravimetric capacity of 4200 mA g^{-1}, the practical application of the Si-based anodes suffers from the huge volume change during the lithiation and de-lithiation processes. A pre-lithiated columnar structured α-Si was proposed as a promising anode (a surface density of 0.660 mg cm^{-2}) for Li–S batteries to avoid the potential safety problems of lithium metal anode, and 10% LiTFSI and 2% $LiNO_3$(by weight) in DOL:DME (1:1 v/v) were used as an electrolyte but it only delivers a reversible capacity of 384 mAh g^{-1} (60% of the initial capacity) after 60 cycles at 0.2 C between1.5 and 2.5 V.[89] It was expected that the issue would be overcme by using a novel battery system consisting of a silicon nanowire anode, an Li_2S/mesoporous carbon composite cathode, and 1 M LiTFSI in DOL/DME (1:1 v/v) as an electrolyte;[90] however, the discharge capacity dropped nearly 50% of

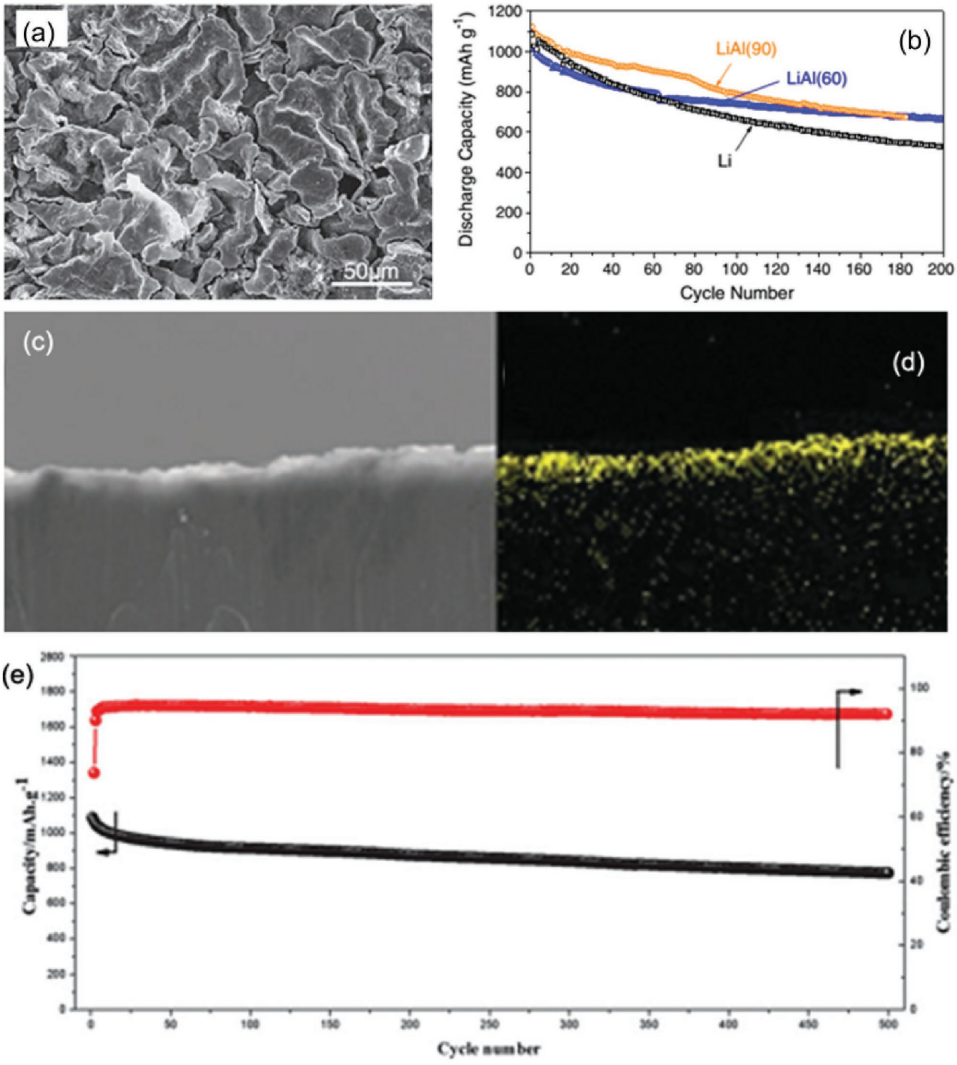

Figure 12. a) SEM image of the Li-Al alloy at 90 °C, b) cycle stability of cells with Li, Li-Al(60) and Li-Al(90) anodes at C/5, c) cross-section morphology, d) EDS mapping element of sulfur, and e) prolonged cycling performance and Coulombic efficiencies at 0.5 C of the Li_3N protected Li anode after 100 cycles. a,b) Reproduced with permission.[80] Copyright 2013, Elsevier. c–e) Reproduced with permission.[83] Copyright 2014, Royal Society of Chemistry.

the initial specific capacity (from 423 mAh g^{-1} to 200 mAh g^{-1}) at a current density of 389 mA g^{-1} between 1.2 and 2.5 V after 20 cycles. A Si-based anode was proposed by Agostini et al. who developed a rechargeable battery based on the combination of an Si–O–C anode with an Li_2S-mesophase carbon microbeads composite in a tetraglyme electrolyte ($LiCF_3SO_3$/TEGDME, a molar ratio of 1:4).[91] The battery delivers a reversible capacity of about 280 mAh g^{-1} at a current density of 233 mA g^{-1} between 0.01 and 3.0 V. Prelithiated silicon nanowire anodes coupled with S/C composite cathodes were served in full Li–S cells with an electrolyte (1 M LiTFSI, 0.25 M $LiNO_3$ in DME/DOL (1:1v/v)), which could deliver a reversible capacity of more than 1200 mAh g^{-1} after 100 cycles between 1.3 and 2.6 V at 0.2 C.[92] A Si microwire array electrode was charged and discharged for 10 cycles with 0.6 mA cm^{-2} between 0.1 and 0.7 V to obtain a pre-lithiated anode.[93] The full cell consisting of a binder-free sulfur infiltrated carbon nanotube cathode combined with pre-lithiated Si microwire anode and an electrolyte (10 mL 0.7 M LiTFSI in DME:DIOX (2:1, v:v)) with 0.1 g Li_2S, 0.1 g S_8 and 0.25 M $LiNO_3$ additives shows a high specific capacity of 800 mAh g^{-1} after 200 cycles at a current of 1.28 mA cm^{-2}. A highly safe Li–S battery using S/C composites as cathode, electrochemically prelithiated Si/C microspheres as an anode, and a room temperature ionic liquid of 0.5 M LiTFSI in *n*-Methyl-*n*-Allylpyrrolidinium bis(trifluoromethanesulfonyl) imide (RTIL $P1A_3TFSI$) as an electrolyte was constructed.[94] Si/C microspheres were prelithiated at a current density of 50 mA g^{-1} by using Swagelok-type cells consisting of Li foil, glass fiber separator and Si/C microspheres, and a cutoff voltage was 0 V versus Li^+/Li, and 1 M LiTFSI in DOL)/DME (1:1 v/v) was used as an electrolyte. An initial discharge capacity of 1457 mAh g^{-1} and a reversible capacity of 670 mAh g^{-1} after 50 cycles at a current rate of 0.1 C in a voltage range of 0.6–2.4 V was obtained in the as-assembled Li–S battery. Recently, a full

lithium–sulfur cell configuration with a dual-type hybrid sulfur cathode and a lithiated Si/SiO_x nanosphere anode with an optimized liquid electrolyte (1 M LiTFSI, 0.4 M $LiNO_3$ and 0.05 M Li_2S_8 (0.4 M S) in DME/DOL (1:1 v:v)) was demonstrated to minimize the problems associated with an excess amount of lithium metal in a lithium-metal anode.[95] The lithiated Si/SiOx anode maintains almost its original thickness without any cracking after 20 cycles. The full cell delivers a specific capacity of about 750 mAh g^{-1} over 500 cycles with cycling efficiencies of more than 98.2% between 0.8 and 2.8 V, and its energy density is more than double that of the commercially available lithium-ion batteries. A ball-milled mixture of silicon nanoparticles with an average particle size of 100 nm and Timcal Super P carbon blacks was dispersed in a solution of lithiated poly(acrylic acid) in deionized water to prepare an Si-based anode of Li–S batteries.[96] Its electrochemical performance was evaluated in large single layer pouch cells (effective electrode areas of 24 cm^2) with a carbon/sulfur composite cathode and an electrolyte (1 M LiTFSI and 0.25 M $LiNO_3$ in DME/DOL (1:1 v:v)). A reversible discharge capacity of about 400 mAh g^{-1} based on the amount of cathode composite (active material of 5 mg cm^{-2}) and anode (active material of 3.4 mg cm^{-2}) after 50 cycles at a current density of 200 mA g^{-1} between 3.5 and 1 V was obtained.

Sn alloys experience a small volume change and a theoretical specific capacity of 990 mAh g^{-1}, and have been evaluated as anode materials for Li–S batteries. An advanced tin–sulfur full cell was fabricated using an Sn/C (1:1 in weight) anode, an Li_2S/C cathode, and polymer electrolytes containing a polymer membrane ($PEO_{20}LiCF_3SO_3$ + 10 wt%S-ZrO_2) and Li_2S-saturated liquid solution (1 M $LiPF_6$ EC/DMC 1:1).[97] It shows a specific capacity of about 500 mAh g^{-1} over 35 cycles at a current density of 38 mA cm^{-2} g^{-1} between 0.2 and 4.0 V. An Sn–C/Li_2S battery with a PEO-based gel polymer electrolyte prepared by swelling a $PEO_{20}LiCF_3SO_3$–10%S–ZrO_2 membrane for 10 min with 1 M $LiPF_6$ EC:DMC 1:1 solution saturated by Li_2S was investigated, which delivers a capacity of 600 mAh g^{-1} at a current density of 38 mA cm^{-2} g^{-1}, and an average voltage of 2 V.[98] A cell balance could be achieved by combining both the Sn–C anode and the Li_2S–C cathode in the battery structure because the specific capacity of the Li_2S–C cathode matches that of the Sn–C anode very well. A Li/Sn–C composite anode was proposed to be used to resolve the intrinsic safety issues associated with the use of metallic lithium anodes in Li–S batteries.[99] The cell constructed by using a lithium/Sn–C composite anode, a carbyne polysulfide cathode, and a carbonic ester electrolyte (1 M $LiPF_6$ in EC: DEC 1:1) delivers a reversible capacity of 500 mAh g^{-1} after 50 cycles at a current density of 200 mA g^{-1} between 1.0 and 3 V. An Li–B alloy anode was also applied in Li–S batteries due to its unique structure which inhibits the formation of dendritic lithium, lowers the interface impedance and enhances the electrochemical performance of Li–S batteries.[100] The cell with the Li-B alloy anode shows a reversible capacity of 694 mAh g^{-1} at a current density of 100 mA g^{-1} between 1.7 and 2.8 V over 100 cycles. These results show that Li-alloying materials can change Li deposition behavior; the huge volume expansion associated with Li-alloying materials leads to a short cycle life during electrochemical lithiation/delithiation cycling.

Lithium-free anodes (e.g., Si, Sn, C) have been demonstrated to be compatible with sulfur cathodes in overcoming the existing issues of Li–S batteries; however, their relative low theoretical energy densities, the issues of unstable SEI layer and large volumetric expansion, and high cost still limit their practical applications in Li–S batteries. Exploring new environmentally friendly and facile routes to improve the electrochemical performance of Li–S batteries is expected.

4. New Strategies for Protecting Li Metal Anode in Li–S Batteries

In contrast to the strategies mentioned above, recently considerable effort has been devoted to revisiting Li metal protection using various Li-ion conducting materials as a protective coating for Li metal electrodes to resist dendrite formation (**Figure 13**). The strategies summarized in **Table 1** have shown to be very effective in blocking the lithium dendrites. More efforts should be devoted to investigating whether they can mitigate the electrolyte consumption problem associated with Li–S batteries, given the Li metal anode often triggers an unexpected reaction with the dissolved intermediate polysulfide species, leading to the low Coulombic efficiency and short cycle life.

4.1. Inorganic Materials

A large range of different carbon-based materials have been used as the protective layers of Li metal anodes including interconnected hollow carbon nanospheres,[101] a carbon nanofiber network,[102] nitrogen-doped graphene sheets,[103] graphite,[104] layered reduced graphene oxide,[105] a 3D porous carbon matrix,[106] an unstacked graphene framework,[107] and a 3D graphene@Ni scaffold.[108] Carbon-based materials are the ideal interfacial layer for the Li metal anode because of their chemical stability in a highly reducing environment, strong mechanical flexibility, and excellent electrical conductivity.

The interfacial layer of hollow carbon nanospheres could suppress the dendrite formation of Li metal anodes up to a practical current density of 1 mA cm^{-2} during charge and discharge cycles. The hollow carbon nanospheres were synthesized via a template synthesis method. An obtained thin film of interconnected hemispherical carbon nanospheres was peeled off from Cu foil and pressed onto the Li metal anode for the electrode fabrication. A stable SEI on the hollow carbon spheres was formed by first cycling the batteries. The corresponding cell with an $LiFePO_4$ cathode and an electrolyte (1 M LiTFSI, 100 × 10–3 M Li_2S_8 and 1% $LiNO_3$ in DME/DOL (1:1 v:v)) shows a high Coulombic efficiency (>99%) over 150 cycles.[101] No dendritic Li metal was observed when the Cu current collector covered with the 3D carbon nanofiber network pieces (1.5 cm^{-2}, 2.8 mg) was synthesized by a vacuum filtration method.[102] The current density of the cycling tests is 1.0 mA·cm^{-2} for discharging (1 h) and charging (1.0 V), and the higher current density is 2.0 mA·cm^{-2} for discharging (0.5 h) and charging (1.0 V). An improved Coulombic efficiency of 99.9% for 300 cycles at a current density of 1.0 and 2.0 mA cm^{-2} could be attributed

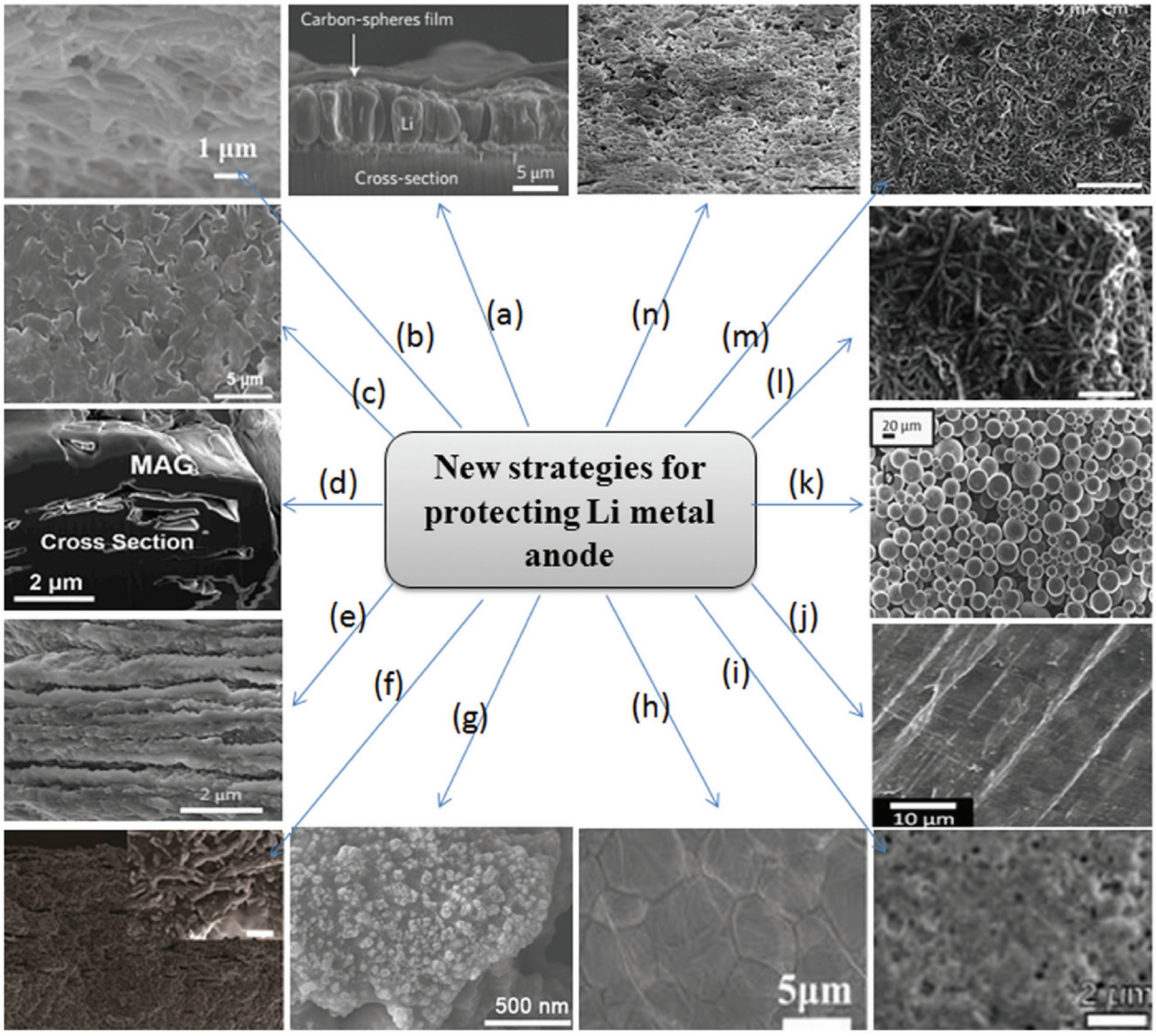

Figure 13. SEM images of the Li metal anodes protected by the different strategies: a) Hollow carbon nanospheres modification with Li-metal deposition, b) 3D carbon nanofiber network/Li-metal anode, c) nitrogen-doped few-layer graphene/Li-metal anode, d) graphite/Li-metal anode, e) layered Li-reduced graphene oxide anode, f) modified carbon fiber network/Li anode, g) graphene/ Li anode, h) 3D graphene@Ni foam/Li anode, i) h-BN protected Li anode, j) ALD Al_2O_3-protected Li anode, k) coated lithium powder anode after cycles, l) 3D oxidized polyacrylonitrile nanofiber/Li anode, m) Li-coated polyimide matrix after 10 cycles, and n) Li deposited on the 3D Cu foil with a submicrometer skeleton. a) Reproduced with permission.[101] Copyright 2014, Nature Publishing Group. b) Reproduced with permission.[102] Copyright 2016, Springer. c) Reproduced with permission.[103] Copyright 2016, American Chemical Society. d) Reproduced with permission.[104] Copyright 2016, Elsevier. e) Reproduced with permission.[105] Copyright 2016, Nature Publishing Group. f) Reproduced with permission.[106] Copyright 2016, National Academy of Sciences. g) Reproduced with permission.[107] Copyright 2016, Wiley-VCH. h) Reproduced with permission.[108] Copyright 2016, American Chemical Society. i) Reproduced with permission.[109] Copyright 2014, American Chemical Society. j) Reproduced with permission.[110] Copyright 2015, American Chemical Society. k) Reproduced with permission.[113] Copyright 2014, Wiley-VCH. l) Reproduced with permission.[114] Copyright 2015, American Chemical Society. m) Reproduced with permission.[115] Copyright 2016, Nature Publishing Group. n) Reproduced with permission.[116] Copyright 2015, Nature Publishing Group.

to the large surface area and good flexibility of the 3D carbon nanofiber network-based anodes.

The island-type, nitrogen-doped graphene coated Cu substrates as electrodes for Li metal storage exhibit stable voltage profiles and excellent efficiency retention over 100 cycles at a current density of 2 mA cm^{-2} in an electrolyte (1 M LiTFSi in DME: DIOX (1:1, vol%)) without additives between −1.0 and 2.0 V,[103] because it could limit the initial Li metal nucleation and growth. It is concluded that the interlayers of graphene sheets play the role of a seed site for the initial Li metal nucleation, and Li ions are first inserted into them during the charge process. Li metal nucleates and grows between the nitrogen-doped graphene sheets, and its growth in other areas on the Cu foil could be inhibited by the insulating PVDF layers. Therefore, Li metal fills the space between the graphene sheet islands and grows on all the electrode surfaces to prevent Li dendrite

Table 1. Summary of various new potential strategies for protecting Li metal anode.

Classification of the protective coating	Method	Cycle performance	Ref.
Interconnected amorphous hollow carbon nanospheres	Vertical deposition+evaporating(400 °C)	≈99% /1 mA cm^{-2}/150 cycles	[101]
3D carbon nanofiber network	3000 °C procedure+vacuum filtration	1 mAh cm^{-2}/≈99.9%/1 mA·cm^{-2}/300 cycles	[102]
Nitrogen-doped few-layer graphene sheets	Ammoniamediated hydrothermal process+spin coating	≈100%/2 mA cm^{-2}/100 cycles	[103]
Graphite	Plating+stripping	≈98.4%/74.4 mA g^{-1}/50 cycles	[104]
Layered reduced graphene oxide	Spark reaction+infusing	≈100%/3 mA cm^{-2}/100 cycles	[105]
3D porous carbon matrix	Carbonization(700 °C)+CVD+melt infusion	1900 mAh cm^{-3}/3mA cm^{-2}/80 cycles	[106]
Unstacked graphene framework	Co-precipitation reaction+depositing+stripping	5 mAh cm^{-2}/≈93%/2 mA cm^{-2}/800 cycles	[107]
3D graphene@Ni foam	Heating(1000 °C)+HCl leaching	≈92%/1 mA cm^{-2}/100 cycles	[108]
Hexagonal boron nitride	CVD(1000 °C) in argon, hydrogen, and ammonia borane vapor	≈97%/2 mA cm^{-2}/50 cycles	[109]
14 nm thick Al_2O_3	Atomic layer deposition	≈1100 mAh g^{-1}/≈83%/100 cycles (Li–S cell)	[110]
3D glass fiber cloths	Interfacial interaction	≈98%/1 mA cm^{-2}/500 cycles	[111]
A home-made gel polymer electrolyte and a LISICON film	Saturating+coating	446 Wh kg^{-1}/≈100%/100 mA g^{-1}/30 cycles(aqueous electrolyte)	[112]
Organic-coated lithium powder	Pressing	≈94.9%/0.885 mA cm^{-2}/100 cycles	[113]
3D oxidized polyacrylonitrile nanofiber	Electrospinning	≈97.4% /3 mA cm^{-2}/120 cycles	[114]
Polyimide fibers+ZnO	Electrospinning+Atomic layer deposition	≈100% /5 mA cm^{-2}/100 cycles	[115]
3D current collector	Pretreatment+reduction (400 °C, H_2/Ar mixed flow)	≈97% /0.5 mA cm^{-2}/50 cycles	[116]

development. The interior structure of graphite particles with many edge planes and some empty space is found to be favorable for fitting all the deposited Li metal,[104] resulting in good electrochemical performance of hybrid graphite-Li-metal anodes. A current density of 74.4 mA g^{-1} and cutoff voltage 2.5 V was found for the extraction and stripping of Li. The layered reduced graphene oxide with a large surface area and good Li affinity was demonstrated as an effective host for storing Li by molten Li thermal infusion.[105] The layered Li–reduced graphene oxide anode exhibits high flexibility and a small electrode dimensional change (≈20%) at 1 mA cm^{-2} during cycling with stable SEI for improving electrochemical performance of cells. The layered Li-reduced graphene oxide anodes were developed by two key steps consisting of the fabrication of layered reduced graphene oxide films with uniform nanogaps and the infusion of Li into the interlayer gaps. Both $LiCoO_2$ and $Li_4Ti_5O_{12}$ were used as cathodes, and 1 M $LiPF_6$ in EC:DEC (1:1, vol %) solution with 2% vinylene carbonate additive as the carbonate-based electrolytes and 1 M LiTFSI inDOL/DME (1:1 v/v) with 1 wt% $LiNO_3$ as the ether-based electrolytes.

3D porous carbon matrix was proposed to host the Li metal.[106] The Li composite anode prepared by encapsulating the molten Li inside the 3D porous carbon host scaffold provides excellent chemical and mechanical stability toward electrochemical cycling. Li entrapment is regarded as a key step for the fabrication of Li composite anode. The symmetrical cells of the proposed 3D Li/C electrode with an electrolyte (1 M $LiPF_6$ in EC/DEC (1:1 vol %)) could deliver a specific capacity of about 2000 mAh g^{-1} at a current density of 3 mA cm^{-2} over 80 cycles. The unstacked graphene with huge specific surface area (1666 m^2 g^{-1}) as the framework of Li deposited in an LiTFSI(0.75 M LiTFSI in DOL)–LiFSI (1.5 M LiFSI in DME) (2:1,volume ratio) electrolyte was developed.[107] The unstacked graphene based Li metal anode shows excellent performance (a lithiation capacity of 5.0 mAh cm^{-2} and Coulombic efficiency of 93%) on both electrochemical behavior and dendrite inhibition at a current density of 2.0 mA cm^{-2}. In order to restrain the formation and growth of Li dendrites, a 3D graphene@Ni scaffold as current collector has been prepared via chemical vapor deposition growth of graphene on Ni foam.[108] Li deposition on 3D graphene@Ni foam shows a high Coulombic efficiency (> 92%) at the current densities of 1.0 mA cm^{-2} in an electrolyte containing 1 M LiTFSI and 2% $LiNO_3$ in DOL:DME (1:1, v:v), because the 3D porous structure with a high surface area was beneficial in reducing the effective electrode current density, and the surface-coated graphene on the Ni foam acts as an artificial protection layer to suppress the growth of Li dendrites and stabilize the SEI film.

An effective protection layer consisting of atomic crystal layer of hBN to suppress dendrite growth was also reported.[109] The BN layers have excellent chemical stability, flexibility and mechanical strength, resulting from the strong intralayer bonds and ultrathin thickness. Additionally, the small pore diameter within each hexagonal ring only allows the penetration of lithium ions, while blocking the invasion of the chemical species. Li metal deposition occurs between BN layers and Cu to form the BN–Li–Cu sandwich structure. The deposition of Li metal controlled with BN layers and Cu could effectively suppress lithium dendrite formation. The h-BN/Cu electrode shows a high Coulombic efficiency of above 95% over 50 cycles at a current density of 1.0 mA cm^{-2}.

Deposition of Al_2O_3 coatings as the protection layer on the Li metal has been proposed.[110] It is demonstrated that a 14 nm thick layer of Al_2O_3 deposition serves as an effective protection barrier against Li metal corrosion upon exposure to air, sulfur, and organic solvent, leading to a dramatic capacity increase and

good stability of the protected Li metal anodes for up to 100 charge and discharge cycles in Li–S coin cells.

3D glass fiber cloths with large quantities of polar functional groups (Si O, OH, OB) as the separator and interlayer of the Li metal anode have been used to uniformly distribute Li ions on the conventional 2D Cu foil current collector to settle the dendrite issue and stabilize the SEI layer.[111] 3D glass fiber-modified cells show improved Coulombic efficiencies of 91% at a high current density rate of 10.0 mA cm^{-2}. The strong interaction between Li ions and glass fiber cloths plays a key role in inhibiting Li dendrite formation. Considerable Li ions are absorbed by the polar functional groups on the surface of glass fiber cloths to compensate the electrostatic interactions between Li ions and protuberances, preventing the accumulation of Li ions around protuberances. The Li ions finally redistribute within the glass fiber frameworks and epitaxially grow from the former Li layer, leading to a termination of the ripple effect and a dendrite-free morphology of Li deposits. As a result, a superior cycling stability and wettability with electrolyte, an enhanced safety performance, and high Coulombic efficiency is achieved by placing the 3D glass fiber cloths between the separator and anode.

4.2. Organic Materials

Coating layers consisting of a home-made gel polymer electrolyte and an LISICON (Li_2O–Al_2O_3–SiO_2–P_2O_5–TiO_2–GeO_2) film are introduced on lithium metal anodes.[112] $LiMn_2O_4$ was used as a cathode, and a 0.5 mol L^{-1} aqueous Li_2SO_4 solution as the electrolyte, the cells with the coated lithium metal anode deliver a reversible capacity of 115 mAh g^{-1} at a current density of 100 mA g^{-1} between 3.7 and 4.25 V after 30 cycles. It is believed that the home-made gel polymer could maintain the good electrochemical stability of the LISICON film, and only Li^+ ions transfer between Li metal and the coating layer. Therefore, the coated lithium metal is very stable in aqueous electrolytes. Organic coated lithium powder instead of lithium metal foil for the anode was proposed to suppress dendrite formation.[113] The anode was prepared by pressing the coated lithium powder on a current collector of the dendritic copper foil, and 1 M $LiPF_6$ in EC and DEC (1:1,volume ratio) solution used as the electrolyte. The anode shows a high Coulombic efficiency of 96.3 at a current density of 0.354 mA cm^{-2} over 100 cycles.

A novel electrode was designed by placing a 3D oxidized polyacrylonitrile nanofiber network with polar surface functional groups on top of the current collector to protect the Li metal anode for a stable cycling performance.[114] The electronically insulating oxidized polyacrylonitrile nanofiber as a scaffold is able to guide and confine the deposition of Li inside the 3D network, because the polar functional groups serve as the adhesion sites to bind with Li ions in the electrolyte. Also, the polar surface groups of the polymer nanofiber network have a strong affinity with electrolyte. The resulting Li metal has a flat surface and stable cycling of the Li-oxidized polyacrylonitrile anode with an average Coulombic efficiency of 97.4% over 120 cycles in DOL/DME electrolyte (1 M LiTFSI and 2% $LiNO_3$ in 1:1 DME/DOL) at a current density of 3 mA cm^{-2} for a total of 1 mAh cm^{-2} of lithium.

Polyimide polymer was proposed to be used as a matrix to confine the stripping and plating of Li and sustain a constant anode volume during cycling due to its outstanding chemical stability, heat resistance and mechanical strength.[115] The polyimide fibers were coated using a layer of ZnO to improve the wetting of molten Li on polyimide polymer. The molten Li reacts with ZnO and can be infused into the core-shell polyimide-ZnO matrix to form an Li-coated polyimide polymer matrix anode, after the matrix comes into contact with the molten Li. Compared with the dense bare Li anode, two key factors, including the porous and the nonconducting polymeric matrix, could contribute to the excellent electrochemical performance of the Li-coated polyimide polymer matrix anode. 1 M LiTFSI and 1 wt% $LiNO_3$ in 1:1 w/w DOL/DME or 1 M $LiPF_6$ in 1:1 EC/DEC was employed as the electrolyte, and $Li_4Ti_5O_{12}$ as the cathode to investigate the Coulombic efficiency of the electrode. A high porosity of the electrode with the increased surface area could significantly reduce the effective current density during cycling. The nonconducting polymeric matrix effectively confines Li within the matrix, and the dendrite-free cycling of the anode is obtained. The cell shows a long-term cycling stability and flat voltage profile at a current rate of 5 mA cm^{-2}.

4.3. Metal Current Collectors

Li anode accommodated in the reserved pores of a 3D porous Cu current collector was demonstrated to significantly suppress Li dendrite growth and improve the lifespan of Li-metal anodes, and the 3D current collector with a submicrometer skeleton and high electroactive surface area fabricated from a commercial planar Cu foil via a facial and scalable method.[116] Their submicrometer structure contributes to delivering a high areal capacity and maintaining a good plating and stripping efficiency (ahout 98.5%). A high electroactive area resulted in an accommodation of a high portion of the Li metal inside the 3D current collector and a reduction of the voltage hysteresis and charge transfer resistance of the Li anode. The electrode of the 3D porous Cu current collector shows the efficiency of about 97% at a current rate of 5 mA cm^{-2} over 50 cycles.

4.4. Artificial Solid Electrolyte Interphase Layer

Besides the above-mentioned methods, designing an artificial Li_3PO_4 SEI layer by in situ reaction of polyphosphoric acid (PPA) with Li metal and its native film is another alternative approach to stabilize the interface between the Li and electrolytes.[117] The native film of Li metal is removed by the uniform Li_3PO_4 SEI layer via an in situ treatment process. The artificial Li_3PO_4 SEI layer on the surface of the Li metal could restrain Li dendrite growth and decrease the side reaction between the electrolyte and the Li metal due to its several outstanding characteristics, such as high Young's modulus, high Li-ion conductivity, and excellent chemical stability during the Li deposition and dissolution process without a breakage and repair mechanism. The PPA-Li cell consisting of a $LiFePO_4$ cathode shows a good cycling stability at a current rate of 0.5 mA cm^{-2} between 2.2 and 4.2 V.

The benefits of the new potential strategies discussed above are that they could offer a fundamental and fresh insight into the safe and highly efficient Li metal electrodes and open up new opportunities for the realization of the next-generation high-energy-density battery systems. However, the polysulfide shuttle effect is a serious problem in impeding the practical application of lithium–sulfur batteries. Therefore, more investigation will be required to determine if these anode protective structures can contribute to protect lithium metal against dissolved lithium polysulfides as well. Moreover, understanding the failure mechanism of an Li metal anode is a big challenge, because the dendrite and corrosion problems of the Li metal anode in Li–S batteries are more complex.

5. Up-Scaled Li–S Cells

Most of the above-mentioned strategies are realized in the coin cells at laboratory scale. Little research of scaled-up Li–S batteries has been reported. It is believed that Li–S pouch cells could be an important step to break through the bottleneck of the further development of practical Li–S batteries.[120,121] The Li–S pouch cells (3 by 5 cm) consisting of the anodes of C-coated Si/SiO_x nanospheres (4.3 mg cm^{-2}), the cathodes of MWCNT-S (MWCNT:S = 1:1 wt%, 2.8 mg cm^{-2}), and the electrolyte (0.5 M LiTFSI, and 0.4 M $LiNO_3$ in DOL:DME (1:1 by volume)) were proposed for the study of up-scaling Li–S batteries.[120] The cell delivers a stable capacity of 500 mAh g^{-1} in the voltage range of 1.8–2.7 V (versus Li^+/Li) at 0.5 C after 400 cycles. The initial capacity decay of the pouch cells could be blamed for the volume changes of the C-Si anodes during cycling. Further work will be required to stabilize the C-coated Si/SiO_x nanospheres anodes for the improvement of practical Si–Li–S pouch cells. The Li–S pouch cells with Li metal anodes and C/S composite cathodes were fabricated by a layer-by-layer strategy to investigate their failure mechanism.[121] The electrochemical performance of Li–S pouch cells is greatly influenced by Li metal anode. The Li–S pouch cell shows a rising discharge capacity from 314 to 1030 mAh g^{-1} at 0.1 C between 1.8 and 2.8 V after replacing the cycled Li anode with a fresh Li metal. The pouch cell failure is attributed to the dendrite formation and the induced polarization. Therefore, as a key component of the pouch cells, the rational choice and design of anodes should be a big challenge for the practical Li–S batteries with a long cycling life.

6. Conclusions

Li–S batteries have been studied for 40 years, and great achievements have been made in the development of new strategies to stabilize Li metal anode in Li–S batteries within the last six years. These strategies in the fabrication of new generation battery systems are expected to enhance the performance of practical Li–S batteries.

The dendrite formation and safety concerns associated with the lithium anode still pose significant challenges preventing commercialization of Li–S batteries. The protection of Li anode is very important in suppressing Li dendrite growth, blocking the unfavorable reaction between soluble polysulfides with Li, and improving the deposition efficiency of Li. Inserting an interlayer between the separator and electrode was found to be effective in decreasing the escape of the polysulfides from the sulfur electrode in Li–S batteries. The novel battery separators, including the modified separator and multifunctional separator, are beneficial in avoiding the formation of lithium dendrites and promoting a long cycling life. The components of the electrolytes, such as solvents, Li salts, and additives, show the significant influence on the chemical compositions, ionic conductivities, and mechanical properties of the SEI layers. Solution-free solid state electrolytes are advanced to reduce the dissolution and shuttle of polysulfides to further stabilize the Li anode. Rational designs of current collectors and artificial protection films not only facilitate rapid ion and electron transport, but also are able to restrain the formation and growth of Li dendrites. Using non-Li materials (such as carbon, Si, and metal alloy) as alternative anode to replace Li metal anode should be one key point to stabilize the long-term cycle stability of lithiated Li_2S-based rechargeable batteries. These strategies to protect Li metal anode may be extended to other rechargeable batteries, including Zn, Na, K, Cu, Ag, and Sn. Additionally, developing a suitable cathode is also one of the key methods to address the main challenges of Li–S systems. Therefore, a systematic approach, including electrode design, separator modification and electrolyte tailoring are required to ensure a high-energy-density system for Li–S batteries. While the rechargeable Li–S batteries could become the most promising high-energy-density system for next-generation electrical energy storage, a commercialization of this battery is still a big challenge.

Acknowledgements

The authors acknowledge financial support from the Science and Technology Program of Guangzhou, China (grant no. 201607010110), Science and Technology Planning Project of Guangdong Province, China (grant no. 2016A010104014), Chinese Nature Science Fundation NSFC (51420105002), as well as the Discovery program from the Australian Research Council.

Conflict of Interest

The authors declare no conflict of interest.

Keywords

anodes, lithium metals, lithium sulfur batteries, protection, recent progresses

Received: January 26, 2017
Revised: March 15, 2017
Published online:

[1] A. Rosenman, E. Markevich, G. Salitra, D. Aurbach, A. Garsuch, F. F. Chesneau, *Adv. Energy Mater.* **2015**, *5*, 1500212.
[2] P. G. Bruce, S. A. Freunberger, L. J. Hardwick, J. M. Tarascon, *Nat. Mater.* **2012**, *11*,19.

[3] A. Manthiram, Y. Z. Fu, S. H. Chung, C. X. Zu, Y. S. Su, *Chem. Rev.* **2014**, *114*, 11751.
[4] R. Xu, I. Belharouak, J. C. M. Li, X. F. Zhang, I. Bloom, J. Bareño, *Adv. Energy Mater.* **2013**, *3*, 833.
[5] D. W. Wang, Q. C. Zeng, G. M. Zhou, L. C. Yin, F. Li, H. M. Cheng, I. R. Gentle, G. Q. M. Lu, *J. Mater. Chem. A* **2013**, *1*, 9382.
[6] X. Fang, H. S. Peng, *Small* **2015**, *11*, 1488.
[7] R. G. Cao, W. Xu, D. P. Lv, J. Xiao, J. G. Zhang, *Adv. Energy Mater.* **2015**, *5*, 1402273.
[8] A. Manthiram, Y. Z. Fu, Y. S. Su, *Acc. Chem. Res.* **2013**, *46*, 1125.
[9] Z. W. Seh, Y. M. Sun, Q. F. Zhang, Y. Cui, *Chem. Soc. Rev.* **2016**, *45*, 5605.
[10] R. J. Chen, T. Zhao, F. Wu, *Chem. Commun.* **2015**, *51*, 18.
[11] G. Y. Xu, B. Ding, J. Pan, P. Nie, L. F. Shen, X. G. Zhang, *J. Mater. Chem. A* **2014**, *2*, 12662.
[12] M. Wild, L. O'Neill, T. Zhang, R. Purkayastha, G. Minton, M. Marinescu, G. J. Offe, *Energy Environ. Sci.* **2015**, *8*, 3477.
[13] Y. X. Yin, S. Xin, Y. G. Guo, L. J. Wan, *Angew. Chem., Int. Ed.* **2013**, *52*, 13186.
[14] Y. S. Su, A. Manthiram, *Nat. Commun.* **2012**, *3*, 1166.
[15] J. G. Wang, Y. Yang, F. Y. Kang, *Electrochim. Acta* **2015**, *168*, 271.
[16] Y. X. Yang, W. Sun, J. Zhang, X. Y. Yue, Z. H. Wang, K. N. Sun, *Electrochim. Acta* **2016**, *209*, 691.
[17] L. Wang, Z. Yang, H. G. Nie, C. C. Gu, W. X. Hua, X. J. Xu, X. Chen, Y. Chen, S. M. Huang, *J. Mater. Chem. A* **2016**, *4*, 15343.
[18] Z. H. Wang, J. Zhang, Y. X. Yang, X. Y. Yue, X. M. Hao, W. Sun, D. Rooney, K. N. Sun, *J. Power Sources* **2016**, *329*, 305.
[19] Z. B. Xiao, Z. Yang, L. Wang, H. G. Nie, M. Zhong, Q. Q. Lai, X. J. Xu, L. J. Zhang, S. M. Huang, *Adv. Mater.* **2015**, *27*, 2891.
[20] Y. S. Su, A. Manthiram, *Chem. Commun.* **2012**, *48*, 8817.
[21] H. M. Kim, J. Y. Hwang, A. Manthiram, Y. K. Sun, *ACS Appl. Mater. Interfaces* **2016**, *8*, 983.
[22] J. Q. Huang, B. Zhang, Z. L. Xu, S. Abouali, M. A. Garakani, J. Q. Huang, J. K. Kim, *J. Power Sources* **2015**, *285*, 43.
[23] X. G. Han, Y. H. Xu, X. Y. Chen, Y. C. Chen, N. Weadock, J. Y. Wan, H. L. Zhu, Y. L. Liu, H. Q. Li, G. Rubloff, C. S. Wang, L. B. Hu, *Nano Energy* **2013**, *2*, 1197.
[24] Z. L. Ma, Z. Li, K. Hu, D. D. Liu, J. Huo, S. Y. Wang, *J. Power Sources* **2016**, *325*, 71.
[25] X. F. Wang, Z. X. Wang, L. Q. Chen, *J. Power Sources* **2013**, *242*, 65.
[26] G. Q. Ma, Z. Y. Wen, J. Jin, M. F. Wu, X. W. Wu, J. C. Zhang, *J. Power Sources* **2014**, *267*, 542.
[27] G. Q. Ma, Z. Y. Wen, Q. S. Wang, C. Shen, P. Peng, J. Jin, X. W. Wu, *J. Power Sources* **2015**, *273*, 511.
[28] N. Yan, X. F. Yang, W. Zhou, H. Z. Zhang, X. F. Li, H. M. Zhang, *RSC Adv.* **2015**, *5*, 26273.
[29] C. Huang, J. Xiao, Y. Y. Shao, J. M. Zheng, W. D. Bennett, D. P. Lu, L. V. Saraf, M. Engelhard, L. W. Ji, J. G. Zhang, X. L. Li, G. L. Graff, J. Liu, *Nat. Commun.* **2014**, *5*, 3015.
[30] H. B. Yao, K. Yan, W. Y. Li, G. Y. Zheng, D. S. Kong, Z. W. Seh, V. K. Narasimhan, Z. Liang, Y. Cui, *Energy Environ. Sci.* **2014**, *7*, 3381.
[31] C. H. Chang, S. H. Chung, A. Manthiram, *Small* **2016**, *12*, 174.
[32] G. M. Zhou, L. Li, D. W. Wang, X. Y. Shan, S. F. Pei, F. Li, H. M. Cheng, *Adv. Mater.* **2015**, *27*, 641.
[33] A. Vizintin, M. U. M. Patel, B. Genorio, R. Dominko, *ChemElectroChem* **2014**, *1*, 1040.
[34] S. H. Chung, A. Manthiram, *Adv. Funct. Mater.* **2014**, *24*, 5299.
[35] J. Balach, T. Jaumann, M. Klose, S. Oswald, J. Eckert, L. Giebeler, *J. Power Sources* **2016**, *303*, 317.
[36] X. Y. Zhou, Q. C. Liao, J. J. Tang, T. Bai, F. Chen, J. Yang, *J. Electroanal. Chem.* **2016**, *768*, 55.
[37] J. Q. Huang, Q. Zhang, H. J. Peng, X. Y. Liu, W. Z. Qian, F. Wei, *Energy Environ. Sci.* **2014**, *7*, 347.
[38] W. L. Cai, G. R. Li, F. He, L. M. Jin, B. H. Liu, Z. P. Li, *J. Power Sources* **2015**, *283*, 524.
[39] F. Wu, Y. S. Ye, R. J. Chen, J. Qian, T. Zhao, L. Li, W. H. Li, *Nano Lett.* **2015**, *15*, 7431.
[40] Z. Y. Zhang, Y. Q. Lai, Z. Zhang, K. Zhang, J. Li, *Electrochim. Acta* **2014**, *129*, 55.
[41] W. Li, J. Hicks-Garner, J. Wang, J. Liu, A. F. Gross, E. Sherman, J. Graetz, J. J. Vajo, P. Liu, *Chem. Mater.* **2014**, *26*, 3403.
[42] X. Y. Qian, L. N. Jin, D. Zhao, X. L. Yang, S. W. Wang, X. Q. Shen, D. W. Rao, S. S. Yao, Y. Y. Zhou, X. M. Xi, *Electrochim. Acta* **2016**, *192*, 346.
[43] H. Tang, S. S. Yao, J. L. Mi, X. Wu, J. L. Hou, X. Q. Shen, *Mater. Lett.* **2017**, *186*, 127.
[44] R. S. Song, R. P. Fang, L. Wen, Y. Shi, S. G. Wang, F. Li, *J. Power Sources* **2016**, *301*, 179.
[45] Q. S. Wang, Z. Y. Wen, J. H. Yang, J. Jin, X. Huang, X. W. Wu, J. D. Han, *J. Power Sources* **2016**, *306*, 347.
[46] G. M. Zhou, L. Li, D. W. Wang, X. Y. Shan, S. F. Pei, F. Li, H. M. Cheng, *Adv. Mater.* **2015**, *27*, 641.
[47] J. D. Zhu, M. Yanilmaz, K. Fu, C. Chen, Y. Lu, Y. Q. Ge, D. Kim, X. W. Zhang, *J. Membr. Sci.* **2016**, *504*, 89.
[48] S. Y. Bai, X. Z. Liu, K. Zhu, S. C. Wu, H. S. Zhou, *Nat. Energy* **2016**, *1*, 16094.
[49] W. Luo, L. H. Zhou, K. Fu, Z. Yang, J. Y. Wan, M. Manno, Y. G. Yao, H. L. Zhu, B. Yang, L. B. Hu, *Nano Lett.* **2015**, *15*, 6149.
[50] J. Scheers, S. Fantini, P. Johansson, *J. Power Sources* **2014**, *255*, 204.
[51] S. S. Zhang, *Electrochim. Acta* **2012**, *70*, 344.
[52] D. Aurbach, E. Pollak, R. Elazari, G. Salitra, C. S. Kelley, J. Affinito, *J. Electron. Mater.* **2009**, *156*, A694.
[53] J. S. Kim, T. H. Hwang, B. G. Kim, J. Min, J. W. Choi, *Adv. Funct. Mater.* **2014**, *24*, 5359.
[54] X. Liang, Z. Wen, Y. Liu, M. Wu, J. Jin, H. Zhang, X. Wu, *J. Power Sources* **2011**, *196*, 9839.
[55] S. Z. Xiong, X. Kai, X. B. Hong, Y. Diao, *Ionics* **2012**, *18*, 249.
[56] C. X. Zu, A. Manthiram, *J. Phys. Chem. Lett.* **2014**, *5*, 2522.
[57] F. Wu, J. Qian, R. J. Chen, J. Lu, L. Li, H. M. Wu, J. Z. Chen, T. Zhao, Y. S. Ye, K. Amine, *ACS Appl. Mater. Interfaces* **2014**, *6*, 15542.
[58] Z. Lin, Z. C. Liu, W. J. Fu, N. J. Dudney, C. D. Liang, *Adv. Funct. Mater.* **2013**, *23*, 1064.
[59] H. Kim, F. X. Wu, J. T. Lee, N. K. Nitta, H. T. Lin, M. Oschatz, W. Cho, S. Kaskel, O. Borodin, G. Yushin, *Adv. Energy Mater.* **2015**, *5*, 1401792.
[60] S. Z. Xiong, K. Xie, E. Blomberg, P. Jacobsson, A. Matic, *J. Power Sources* **2014**, *252*, 150.
[61] L. X. Yuan, J. K. Feng, X. P. Ai, Y. L. Cao, S. L. Chen, H. X. Yang, *Electrochem. Commun.* **2006**, *8*, 610.
[62] F. Wu, Q. Z. Zhu, R. J. Chen, N. Chen, Y. Chen, Y. S. Ye, J. Qian, L. Li, *J. Power Sources* **2015**, *296*, 10.
[63] J. M. Zheng, M. Gu, H. H. Chen, P. Meduri, M. H. Engelhard, J. G. Zhang, J. Liu, J. Xiao, *J. Mater. Chem. A* **2013**, *1*, 8464.
[64] F. Wu, Q. Z. Zhu, R. J. Chen, N. Chen, Y. Chen, L. Li, *Electrochim. Acta* **2015**, *184*, 356.
[65] G. Q. Ma, Z. Y. Wen, J. Jin, M. F. Wu, G. X. Zhang, X. W. Wu, J. C. Zhang, *Solid State Ionics* **2014**, *262*, 174.
[66] M. Barghamadia, A. S. Best, A. I. Bhatt, A. F. Hollenkamp, P. J. Mahon, M. Musameh, T. Rüther, *J. Power Sources* **2015**, *295*, 212.
[67] D. Bresser, S. Passerini, B. Scrosati, *Chem. Commun.* **2013**, *49*, 10545.
[68] M. Liu, D. Zhou, Y. B. He, Y. Z. Fu, X. Y. Qin, C. Miao, H. D. Du, B. H. Li, Q. H. Yang, Z. Q. Lin, T. S. Zhao, F. Y. Kang, *Nano Energy* **2016**, *22*, 278.
[69] J. Hassoun, B. Scrosati, *Adv. Mater.* **2010**, *22*, 5198.

[70] S. S. Jeong, Y. T. Lim, Y. J. Choi, G. B. Cho, K. W. Kim, H. J. Ahn, K. K. Cho, *J. Power Sources* **2007**, *174*, 745.
[71] S. S Zhang, D. T. Tran, *Electrochim. Acta* **2013**, *114*, 296.
[72] M. Nagao, Y. Imade, H. Narisawa, T. Kobayashi, R. Watanabe, T. Yokoi, T. Tatsumi, R. Kanno, *J. Power Sources* **2013**, *222*, 237.
[73] M. Nagao, K. Suzuki, Y. Imade, M. Tateishi, R. Watanabe, T. Yokoi, M. Hirayama, T. Tatsumi, R. Kanno, *J. Power Sources* **2016**, *330*, 120.
[74] A. Hayashi, T. Ohtomo, F. Mizuno, K. Tadanaga, M. Tatsumisago, *Electrochem. Commun.* **2003**, *5*, 701.
[75] T. Yamada, S. Ito, R. Omoda, T. Watanabe, Y. Aihara, M. Agostini, U. Ulissi, J. Hassoun, B. Scrosati, *J. Electrochem. Soc.* **2015**, *162*, A646.
[76] M. Agostini, Y. Aihar, T. Yamada, B. Scrosati, J. Hassoun, *Solid State Ionics* **2013**, *244*, 48.
[77] N. Kamaya, K. Homma, Y. Yamakawa, M. Hirayama, R. Kanno, M. Yonemura, T. Kamiyama, Y. Kato, S. Hama, K. Kawamoto, A. Mitsui, *Nat. Mater.* **2011**, *10*, 682.
[78] J. E. Trevey, Y. S. Jung, S. H. Lee, *Electrochim. Acta* **2011**, *56*, 4243.
[79] I. Villalueng, K. H. Wujcik, W. Tong, D. Devaux, D. H. C. Wong, J. M. DeSimone, N. P. Balsara, *Proc. Natl. Acad. Sci. USA* **2016**, *113*, 52.
[80] H. Kim, J. T. Lee, D. C. Lee, M. Oschatz, W. Cho, S. Kaskel, G. Yushin, *Electrochem. Commun.* **2013**, *36*, 38.
[81] M. F. Wu, Z. Y. Wen, J. Jin, Y. M. Cui, *Electrochim. Acta* **2013**, *103*, 199.
[82] Y. M. Lee, N. S. Choi, J. H. Park, J. K. Park, *J. Power Sources* **2003**, *119*, 964.
[83] G. Q. Ma, Z. Y. Wen, M. F. Wu, C. Shen, Q. S. Wang, J. Jin, X. W. Wu, *Chem. Commun.* **2014**, *50*, 14209.
[84] M. Agostini, B. Scrosati, J. Hassoun, *Adv. Energy Mater.* **2015**, *5*, 1500481.
[85] J. Brückner, S. Thieme, F. Böttger-Hiller, I. Bauer, H. T. Grossmann, P. Strubel, H. Althues, S. Spange, S. Kaskel, *Adv. Funct. Mater.* **2014**, *24*, 1284.
[86] S. Y. Zheng, Y. Chen, Y. H. Xu, F. Yi, Y. J. Zhu, Y. H. Liu, J. Yang, C. S. Wang, *ACS Nano* **2013**, *12*, 10995.
[87] F. Xu, X. Li, F. Xiao, S. Z. Xu, X. P. Zhang, P. He, H. S. Zhou, *Adv. Perform. Mater.* **2016**, *31*, 517.
[88] J. Hassoun, J. Kim, D. J. Lee, H. G. Jung, S. M. Lee, Y. K. Sun, B. Scrosati, *J. Power Sources* **2012**, *202*, 308.
[89] R. Elazari, G. Salitra, G. Gershinsky, A. Garsuch, A. Panchenko, D. Aurbach, *Electrochem. Commun.* **2012**, *14*, 21.
[90] Y. Yang, M. T. McDowell, A. Jackson, J. J. Cha, S. S. Hong, Y. Cui, *Nano Lett.* **2010**, *10*, 1486.
[91] M. Agostini, J. Hassoun, J. Liu, M. Jeong, H. Nara, T. Momma, T. Osaka, Y. K. Sun, B. Scrosati, *ACS Appl. Mater. Interfaces* **2014**, *6*, 10924.
[92] A. Krause, S. Dörfler, M. Piwko, F. M. Wisser, T. Jaumann, E. Ahrens, L. Giebeler, H. Althues, S. Schädlich, J. Grothe, A. Jeffery, M. Grube, J. Brückner, J. Martin, J. Eckert, S. Kaskel, T. Mikolajick, W. M. Weber, *Sci. Rep.* **2016**, *6*, 27982.
[93] M. Hagen, E. Quiroga-González, S. Dörfler, G. Fahrer, J. Tübke, M. J. Hoffmann, H. Althues, R. Speck, M. Krampfert, S. Kaskel, H. Föll, *J. Power Sources* **2014**, *248*, 1058.
[94] Y. Yan, Y. X. Yin, S. Xin, J. Su, Y. G. Guo, L. J. Wan, *Electrochim. Acta* **2013**, *91*, 58.
[95] S. K. Lee, S. M. Oh, E. Park, B. Scrosati, J. Hassoun, M. Park, Y. J. Kim, H. Kim, I. Belharouak, Y. K. Sun, *Nano Lett.* **2015**, *15*, 2863.
[96] M. Weinberger, M. Wohlfahrt-Mehrens, *Electrochim. Acta* **2016**, *191*, 124.
[97] J. Hassoun, B. Scrosati, *Angew. Chem., Int. Ed.* **2010**, *49*, 2371.
[98] J. Hassoun, Y. K. Sun, B. Scrosati, *J. Power Sources* **2011**, *196*, 343.
[99] B. C. Duan, W. K. Wang, A. B. Wang, Z. B. Yu, H. L. Zhao, Y. S. Yang, *J. Mater. Chem. A* **2014**, *2*, 308.
[100] X. L. Zhang, W. K. Wang, A. B. Wang, Y. Q. Huang, K. G. Yuan, Z. B. Yu, J. Y. Qiu, Y. S. Yang, *J. Mater. Chem. A* **2014**, *2*, 11660.
[101] G. Y. Zheng, S. W. Lee, Z. Liang, H. W. Lee, K. Yan, H. B. Yao, H. T. Wang, W. Y. Li, S. Chu, Y. Cui, *Nat. Nanotechol.* **2014**, *9*, 618.
[102] A. Y. Zhang, X. Fang, C. F. Shen, Y. H. Liu, C. W. Zhou, *Nano Res.* **2016**, *9*, 3428.
[103] H. K. Kang, S. G. Woo, J. H. Kim, J. S. Yu, S. R. Lee, Y. J. Kim, *ACS Appl. Mater. Interfaces* **2016**, *8*, 26895.
[104] Y. M. Sun, G. Y. Zheng, Z. W. Seh, N. Liu, S. Wang, J. Sun, H. R. Lee, Y. Cui, *Chem* **2016**, *1*, 287.
[105] D. C. Lin, Y. Y. Liu, Z. Liang, H. W. Lee, J. Sun, H. T. Wang, K. Yan, J. Xie, Y. Cui, *Nat. Nanotechol.* **2016**, *11*, 626.
[106] Z. Liang, D. C. Lin, J. Zhao, Z. D. Lu, Y. Y. Liu, C. Liu, Y. Y. Lu, H. T. Wang, K. Yan, X. Y. Tao, Y. Cui, *Proc. Natl. Acad. Sci. USA* **2016**, *113*, 2862.
[107] R. Zhang, X. B. Cheng, C. Z. Zhao, H. J. Peng, J. L. Shi, J. Q. Huang, J. F. Wang, F. Wei, Q. Zhang, *Adv. Mater.* **2016**, *28*, 2155.
[108] K. Y. Xie, W. F. Wei, K. Yuan, W. Lu, M. Guo, Z. H. Li, Q. Song, X. G. Liu, J. G. Wang, C. Shen, *ACS Appl. Mater. Interfaces* **2016**, *8*, 26091.
[109] K. Yan, H. W. Lee, T. Gao, G. Y. Zheng, H. B. Yao, H. T. Wang, Z. D. Lu, Y. Zhou, Z. Liang, Z. F. Liu, S. Chu, Y. Cui, *Nano Lett.* **2014**, *14*, 6016.
[110] A. C. Kozen, C. F. Lin, A. J. Pearse, M. A. Schroeder, X. G. Han, L. B. Hu, S. B. Lee, G. W. Rubloff, M. Noked, *ACS Nano* **2015**, *9*, 5884.
[111] X. B. Cheng, T. Z. Hou, R. Zhang, H. J. Peng, C. Z. Zhao, J. Q. Huang, Q. Zhang, *Adv. Mater.* **2016**, *28*, 2888.
[112] X. J. Wang, Y. Y. Hou, Y. S. Zhu, Y. P. Wu, R. Holze, *Sci. Rep.* **2013**, *3*, 1401.
[113] J. Heine, S. Krüger, C. Hartnig, U. Wietelmann, M. Winter, P. Bieker, *Adv. Energy Mater.* **2014**, *4*, 1300815.
[114] Z. Liang, G. Y. Zheng, C. Liu, N. Liu, W. Y. Li, K. Yan, H. B. Yao, P. C. Hsu, S. Chu, Y. Cui, *Nano Lett.* **2015**, *15*, 2910.
[115] Y. Y. Liu, D. C. Lin, Z. Lian, J. Zhao, K. Yan, Y. Cui, *Nat. Commun.* **2016**, *7*, 10992.
[116] C. P. Yang, Y. X. Yin, S. F. Zhang, N. W. Li, Y. G. Guo, *Nat. Commun.* **2015**, *6*, 8058.
[117] N. W. Li, Y. X. Yin, C. P. Yang, Y. G. Guo, *Adv. Mater.* **2016**, *28*, 1853.
[118] Z. X. Hao, L. X. Yuan, Z. Li, J. Liu, J. W. Xiang, C. Wu, R. Zeng, Y. H. Huang, *Electrochim. Acta* **2016**, *200*, 197.
[119] A. Basile, A. I. Bhatt, A. P. O'Mullane, *Nat. Commun.* **2016**, *7*, 11794.
[120] H. S. Kang, E. Park, J. Y. Hwang, H. Kim, D. Aurbach, A. Rosenman, Y. K. Sun, *Adv. Mater. Technol.* **2016**, *1*, 1600052.
[121] X. B. Cheng, C. Yan, J. Q. Huang, P. Li, L. Zhu, L. D. Zhao, Y. Y. Zhang, W. C. Zhu, S. T. Yang, Q. Zhang, *Energy Storage Mater.* **2017**, *6*, 18.